Supplement of Atmos. Chem. Phys., 24, 3989–4000, 2024
https://doi.org/10.5194/acp-24-3989-2024-supplement

Atmospheric Chemistry and Physics
Open Access
EGU

Supplement of

Molecular-level study on the role of methanesulfonic acid in iodine oxoacid nucleation

Jing Li et al.

Correspondence to: An Ning (anning@bit.edu.cn) and Xiuhui Zhang (zhangxiuhui@bit.edu.cn)

Table of Contents

Supplementary Methods

Multi-step cluster conformational searching method.

The definition of cluster formation rate.

Uncertainty analysis.

Figure S1. Number of hydrogen bonds (HBs) and halogen bonds (XBs) in the HIO_3-HIO_2 clusters and HIO_3-HIO_2-MSA clusters.

Figure S2. The ESP-mapped molecular vdW surfaces of the $(HIO_3)_1(HIO_2)_3(MSA)_1$ cluster. The red region is the electron-deficient region, and the blue region is the electron-rich region.

Figure S3. The branch ratio of different flux out of HIO_3-HIO_2-MSA-based system at **(a)** T = 278 K, $[HIO_3] = 1.0 \times 10^6$, $[HIO_2] = 2.0 \times 10^4$, [MSA] = $10^6 – 10^8$ molec. cm^{-3}, and **(b)** T = 278 K, $[HIO_3] = 10^6 – 10^8$, $[HIO_2] = 2.0 \times 10^4 – 2.0 \times 10^6$, $[MSA] = 1.0 \times 10^7$ molec. cm^{-3}.

Figure S4. The branch ratio of different flux out of HIO_3-HIO_2-MSA-based system at **(a)** T = 268 K, $[HIO_3] = 1.0 \times 10^6$, $[HIO_2] = 2.0 \times 10^4$, [MSA] = $10^6 – 10^8$ molec. cm^{-3}, **(b)** T = 268 K, $[HIO_3] = 10^6 – 10^8$, $[HIO_2] = 2.0 \times 10^4 – 2.0 \times 10^6$, $[MSA] = 1.0 \times 10^7$ molec. cm^{-3}, and **(c)** T = 268 K, $[HIO_3] = 10^6 – 10^8$, $[HIO_2] = 2.0 \times 10^4 – 2.0 \times 10^6$, $[MSA] = 1.0 \times 10^8$ molec. cm^{-3}.

Figure S5. The Gibbs free energies of formation (ΔG, kcal mol^{-3}) of the growing clusters as a function of growth step in HIO_3-HIO_2-MSA nucleation system at T = 268 K, $[HIO_3] = 1.0 \times 10^6$, $[HIO_2] = 2.0 \times 10^4$, and $[MSA] = 5.0 \times 10^6$ molec. cm^{-3}.

Figure S6. The concentration (molec. cm^{-3}) of stable clusters in HIO_3-HIO_2-MSA system as a function of time, at T = 278 K, CS = 2.0×10^{-3} s^{-1}, $[HIO_3] = 10^6$, $[HIO_2] = 2.0 \times 10^4$, $[MSA] = 5.0 \times 10^6$ molec. cm^{-3}.

Figure S7. Main cluster growth pathway of the HIO_3-HIO_2-MSA nucleating system at T = 278K, CS = 2.0×10^{-3} s^{-1}, (a) [HIO_3] = 1.0×10^7, [HIO_2] = 2.0×10^5, and [MSA] = 1.0×10^7 molec. cm^{-3}, (b) [HIO_3] = 1.0×10^6, [HIO_2] = 2.0×10^4, and [MSA] = 1.0×10^6 molec. cm^{-3}.

Figure S8. Simulated cluster formation rates J (cm^{-3} s^{-1}) against varying atmospheric temperatures (T = 258 – 298 K), CS = 1.0×10^{-2} s^{-1}, [HIO_3] = 1.0×10^7, [HIO_2] = 2.0×10^5, and [MSA] = 1.0×10^7 molec. cm^{-3}.

Figure S9. Simulated cluster formation rates J (cm^{-3} s^{-1}) against varying atmospheric temperatures (T = 258 – 298 K), CS = 1.0×10^{-4} s^{-1}, [HIO_3] = 1.0×10^7, [HIO_2] = 2.0×10^5, and [MSA] = 1.0×10^7 molec. cm^{-3}.

Figure S10. Enhancement strength R of MSA on cluster formation rates at varying precursor concentrations: [HIO_3] = 10^6 – 10^8, [HIO_2] = 2.0×10^4 – 2.0×10^6 molec. cm^{-3}, **(a)** [MSA] = 1.0×10^6 molec. cm^{-3}, **(b)** [MSA] = 1.0×10^7 molec. cm^{-3}, and **(c)** [MSA] = 1.0×10^8 molec. cm^{-3}, T = 278 K, CS = 1.0×10^{-2} s^{-1}.

Figure S11. Enhancement strength R of MSA on cluster formation rates at varying precursor concentrations: [HIO_3] = 10^6 – 10^8, [HIO_2] = 2.0×10^4 – 2.0×10^6 molec. cm^{-3}, **(a)** [MSA] = 1.0×10^6 molec. cm^{-3}, **(b)** [MSA] = 1.0×10^7 molec. cm^{-3}, and **(c)** [MSA] = 1.0×10^8 molec. cm^{-3}, T = 278 K, CS = 1.0×10^{-4} s^{-1}.

Figure S12. Simulated cluster formation rates J (cm^{-3} s^{-1}) against varying [MSA] = 10^6 – 10^7 molec. cm^{-3}, at T = 278 K, CS = 2.0×10^{-3} s^{-1}, [HIO_3] = 1.0×10^6, [HIO_2] = 2.0×10^4 molec. cm^{-3}.

Figure S13. The Gibbs free energies of cluster formation (ΔG, kcal mol^{-1}) based on the main clustering pathway in HIO_3-MSA and HIO_3-HIO_2-MSA nucleation system at T = 278 K, CS = 2.0×10^{-3} s^{-1}, [HIO_3] = 1.0×10^6, [HIO_2] = 2.0×10^4 molec. cm^{-3}.

Figure S14. Comparison with the simulated cluster formation rates (J, cm^{-3} s^{-1}) and field observations at the ambient conditions of **(a)** Réunion (T = 288 K, CS = 2.0×10^{-3} s^{-1}, [HIO_3] = 10^5

– 3.0 × 10^6, [HIO_2] = 2.0 × 10^3 – 6.0 × 10^4, and [MSA] = 10^6 – 10^8 molec. cm^{-3}), **(b)** Mace Head (*T* = 287 K, CS = 2.0 × 10^{-3} s^{-1}, [HIO_3] = 10^7 – 10^8, [HIO_2] = 2.0 × 10^5 – 2.0 × 10^6, and [MSA] = 10^6 – 10^7 molec. cm^{-3}). The orange area, purple line and gray area represent *J*(HIO_3-HIO_2-MSA), *J*(HIO_3-HIO_2), and *J*(Field observation), respectively. [HIO_3]/[HIO_2] is a constant.

Figure S15. Variation of enhancement strength *R* of MSA with **(a)** condensation sink coefficient (CS) and **(b)** sticking factor (SF) for HIO_3-HIO_2-MSA system at *T* = 278 K, [HIO_3] = 1.0 × 10^7, [HIO_2] = 2.0 × 10^5, and [MSA] = 1.0 × 10^7 molec. cm^{-3}.

Figure S16. Cluster formation rate *J* **(a)** and enhancement strength *R* of MSA **(b)** as a function of [MSA] = 10^6 – 10^8 molec. cm^{-3}, with different Gibbs free energy of ΔG_{278K} (black line), ΔG_{278K} + 1 (blue line), ΔG_{278K} – 1 (red line), at *T* = 278 K, CS = 2.0 × 10^{-3} s^{-1}, [HIO_3] = 10^7, [HIO_2] = 2.0 × 10^5 molec. cm^{-3}.

Figure S17. Cluster formation rate *J* (cm^{-3} s^{-1}) as a function of [MSA] = 10^6 – 10^8 molec. cm^{-3}, with different energy of ΔG_{ref} (red line, reference condition), ΔG_{rand} (blue line, randomly assigned ΔG values of all clusters within the potential bias between -1 and 1 kcal mol^{-1}), at *T* = 278 K, CS = 2.0 × 10^{-3} s^{-1}, [HIO_3] = 10^7, [HIO_2] = 2.0 × 10^5 molec. cm^{-3}.

Table S1. The Gibbs formation free energies ΔG_{ref} (kcal mol^{-1}) of the studied HIO_3-HIO_2-MSA clusters at the RICC2/aug-cc-pV(T+d)Z(-PP)//ωB97X-D/6-311++G(3df,3pd) + aug-cc-pVTZ-PP with ECP28MDF (for I) level of theory, *p* = 1 atm and *T* = 258, 268, 278, 288, and 298 K.

Table S2. The bond type, electron density $\rho(r)$ (a.u), Laplacian electron density $\nabla^2\rho(r)$ (a.u.), energy density $H(r)$ at the corresponding bond critical points (BCPs) in the studied HIO_3-HIO_2-MSA-based clusters. The orange balls represent BCPs in the AIM theory analysis. HIO_3, HIO_2, and MSA are the shorthand for iodic acid, iodous acid and methanesulfonic acid, respectively. HB (hydrogen bond), XB (halogen bond).

Table S3. The boundary conditions of ACDC simulations at 258, 268, 278, 288, and 298 K,

respectively.

Table S4. The ratios of HIO_3 monomer collision frequencies versus total evaporation rate coefficients ($\beta C/\Sigma\gamma$) at T = 258, 268, 278, 288, and 298 K. β is the rate coefficient of cluster collision with HIO_3 monomer, and C is the concentration of HIO_3 monomer (1.0×10^6 molec. cm^{-3}).

Table S5. The evaporation rate coefficients (γ, s^{-1}) of the studied clusters at 268 K.

Table S6. The evaporation rate coefficients (γ, s^{-1}) of the studied clusters at 278 K.

Table S7. The total evaporation rate coefficients ($\Sigma\gamma$, s^{-1}) of clusters calculated at 278 K.

Table S8. Cluster formation rate J of HIO_3-HIO_2-MSA system under different Gibbs free energy (ΔG_{278K}, ΔG_{278K} + 1, ΔG_{278K} - 1) at T = 278 K, CS = 2.0×10^{-3} s^{-1}, [HIO_3] = 10^7, [HIO_2] = 2.0×10^5, [MSA] = 10^6 – 10^8 molec. cm^{-3}.

Table S9. Cartesian coordinates of all clusters in the present study at the ωB97X-D/6-311++G(3df,3pd) + aug-cc-pVTZ-PP with ECP28MDF (for I) level of theory.

Supplementary Methods

Multi-step cluster conformational searching method.

First, the artificial bee colony algorithm combined with Universal force field (UFF) (Rappé et al., 1992) was employed to yield more than 7000000 initial configurations for each cluster by ABCluster software (Zhang and Dolg, 2015). Then up to 1000 relatively stable structures were selected to pre-optimized at the PM7 semiempirical method (Stewart, 2013) by MOPAC 2016 (Stewart, 2016). Next, about 100 structures with the lowest energy were selected to further optimized at the ωB97X-D/6-31+G* (for C, H, O and S atoms) + Lanl2DZ (for I atom) level of theory (Elm and Kristensen, 2017) by Gaussian 09 software (Frisch et al., 2009). Finally, the lower-lying 10 isomers were selected and reoptimized at the ωB97X-D function and 6-311++G (3df, 3pd) (for C, H, O and S atoms) + aug-cc-pVTZ-PP with ECP28MDF (for I atom) level of theory to obtain the global minimum one (Francl et al., 1982; Peterson et al., 2003).

The definition of cluster formation rate.

In the ACDC simulation, nucleation generally refers to the formation of relatively stable clusters for which collisions with molecules can be assumed to dominate over cluster evaporation. Accordingly, the cluster formation rate (J) indicates the particle flux out of the studied system. In this case, it is the rate of clusters forming at some specific size (*i.e.* the net flux into the size from all other sizes)(Oona and Tinja, 2020).

According to the Kerminen-Kulmala equation (Kulmala et al., 2012), cluster formation rates for d_2 nm clusters (J_{d_2}) relate to those for d_1 nm clusters (J_{d_1}) by

$$J_{d_1} = J_{d_2} \exp\left\{\gamma\left(\frac{1}{d_1} - \frac{1}{d_2}\right)\frac{\mathrm{CS'}}{\mathrm{GR}_{d_2\text{-}d_1}}\right\},$$

where the parameter γ depends on many factors but can usually be approximated by assuming it to be equal to 0.23 nm^2 m^2 h^{-1}. The $\mathrm{GR}_{d_2\text{-}d_1}$ is the initial cluster growth rate from d_1 to d_2 nm, and CS' represents condensation sink of clusters by preexisting particles. According to the study of Kerminena and Kulmalab (2002), we have converted the CS value to CS' by the following equation (Kerminen and Kulmala, 2002):

$$\mathrm{CS} = 4\pi D_i \mathrm{CS'}$$

where D_i is the diffusion coefficient of the condensing vapor, usually assumed to be sulfuric acid (0.08 cm^{-2} s^{-1}) (Kulmala et al., 2012). When the CS value is 0.002 s^{-1}, the CS' value is 18 m^{-2}.

Therefore, the relationship between the formation rates of simulated clusters ($J_{1.2}$) and observed clusters ($J_{1.5}$) can be written as:

$$J_{1.2} = J_{1.5} \exp\left\{0.23 \times \left(\frac{1}{1.2} - \frac{1}{1.5}\right)\frac{\mathrm{CS'}}{\mathrm{GR}}\right\},$$

where GR was measured to be 3.2 – 4.4 nm·h^{-1} in the 1.1 – 2.0 nm size range during three observed events (Xia et al., 2020; Yu et al., 2019), and CS' value was 18 m^{-2}. Accordingly, the calculated $J_{1.2}$

is 1.1 – 1.2 times of $J_{1.5}$. The observed cluster formation rates for 1.5 nm clusters can be converted to the simulated $J_{1.2}$.

Uncertainty analysis.

Here, the potential uncertainties may stem from ACDC simulations and quantum chemical (QC) calculations, we examined the effect of condensation sink coefficient (CS), sticking factor (SF) and calculated ΔG of clusters on enhancement of MSA to the cluster formation rate. The CS values ranged from 1.0×10^{-4} s^{-1} to 1.0×10^{-2} s^{-1}, covering possible CS in relatively clean and polluted regions (He et al., 2021; Yu et al., 2019). The range of SF was set from 0.1 to 1.0 since sticking probabilities for neutral-neutral collisions between 0.1 and 1.0 (Almeida et al., 2013). Both the CS and SF slightly affect the enhancement of MSA, with limited uncertainty range of CS < 32.5% and SF < 17.1% (Fig. S15). As reported by Kupiainen et al., the differences between the computational (DFT//RI-CC2 method) and experimental ΔG values are about 1 kcal mol^{-1} or less (Kupiainen et al., 2012; Froyd and Lovejoy, 2012). Accordingly, Almedia et al. calculated the uncertainty range of ACDC simulated cluster formation resulting from QC calculations by adjusting the binding energy (±1 kcal mol^{-1}) (Almeida et al., 2013). Further given the consistency of our research framework (DFT//RI-CC2 + ACDC) with Almedia et al. (2013), herein we have performed the uncertainty analysis of R_{MSA} caused by QC calculations through adding or subtracting 1 kcal mol^{-1} from the ΔG (using ΔG_{278K} as a reference). As shown in Table S8 and Fig. S16, adjusting the ΔG_{278K} of clusters by ±1 kcal mol^{-1} resulted in a minor variation in J and R of MSA. Furthermore, given that the potential bias of all clusters may not move in the same direction, we have further randomly assigned ΔG value of each cluster (ΔG_{rand} at 278 K) within its uncertainty range (ΔG_{ref} – 1 kcal mol^{-1} < ΔG_{rand} < ΔG_{ref} + 1 kcal mol^{-1}), where ΔG_{ref} indicates the results from the current quantum chemical

calculations. Using the newly assigned ΔG_{rand}, we have further performed the ACDC simulations to calculate the cluster formation rate (J). Figure S17 presents the results of 500 calculations. The results do not alter the overall trend of the rate variation, and the resulting principal conclusions of this study.

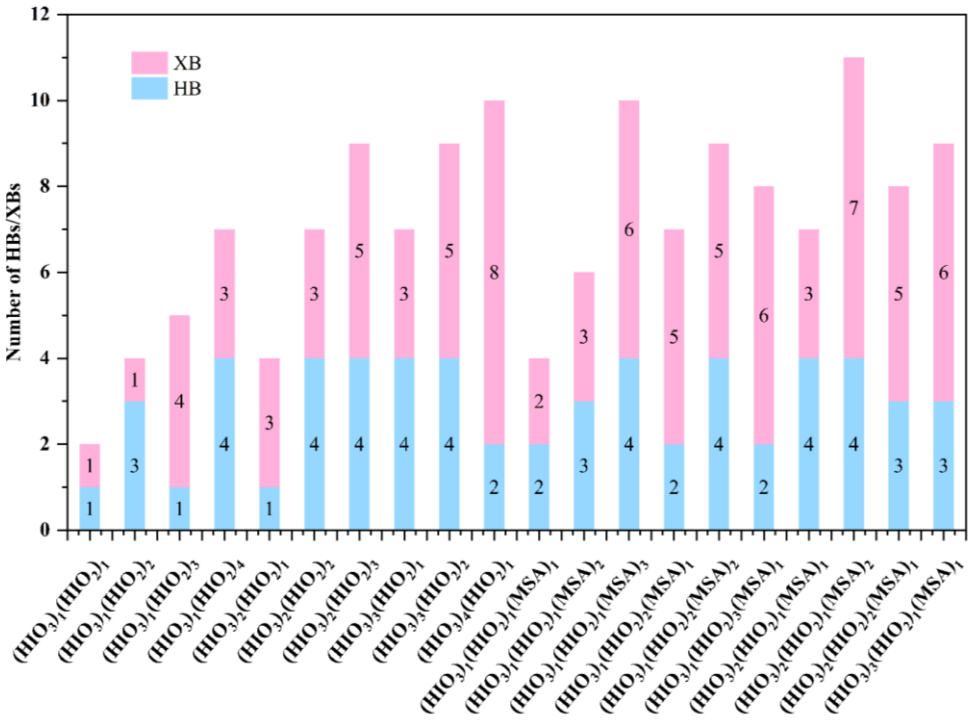

Figure S1. Number of hydrogen bonds (HBs) and halogen bonds (XBs) in the HIO_3-HIO_2 clusters and HIO_3-HIO_2-MSA clusters.

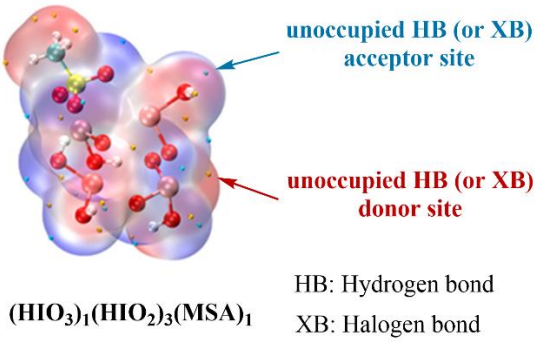

Figure S2. The ESP-mapped molecular vdW surfaces of the $(HIO_3)_1(HIO_2)_3(MSA)_1$ cluster. The red region is the electron-deficient region, and the blue region is the electron-rich region.

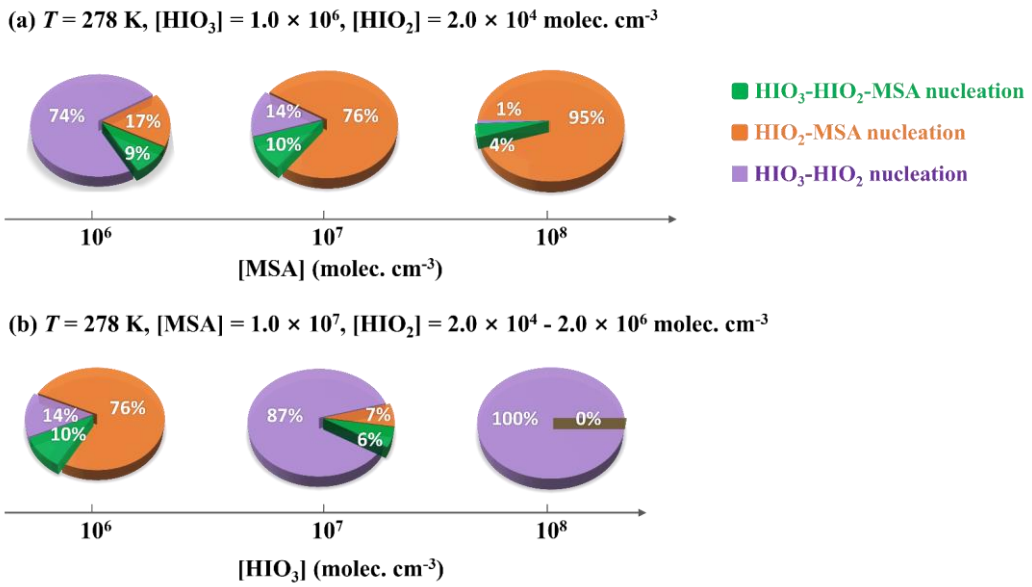

Figure S3. The branch ratio of different flux out of HIO_3-HIO_2-MSA-based system at **(a)** T = 278 K, [HIO_3] = 1.0 × 10^6, [HIO_2] = 2.0 × 10^4, [MSA] = 10^6 – 10^8 molec. cm^{-3}, and **(b)** T = 278 K, [HIO_3] = 10^6 – 10^8, [HIO_2] = 2.0 × 10^4 – 2.0 × 10^6, [MSA] = 1.0 × 10^7 molec. cm^{-3}.

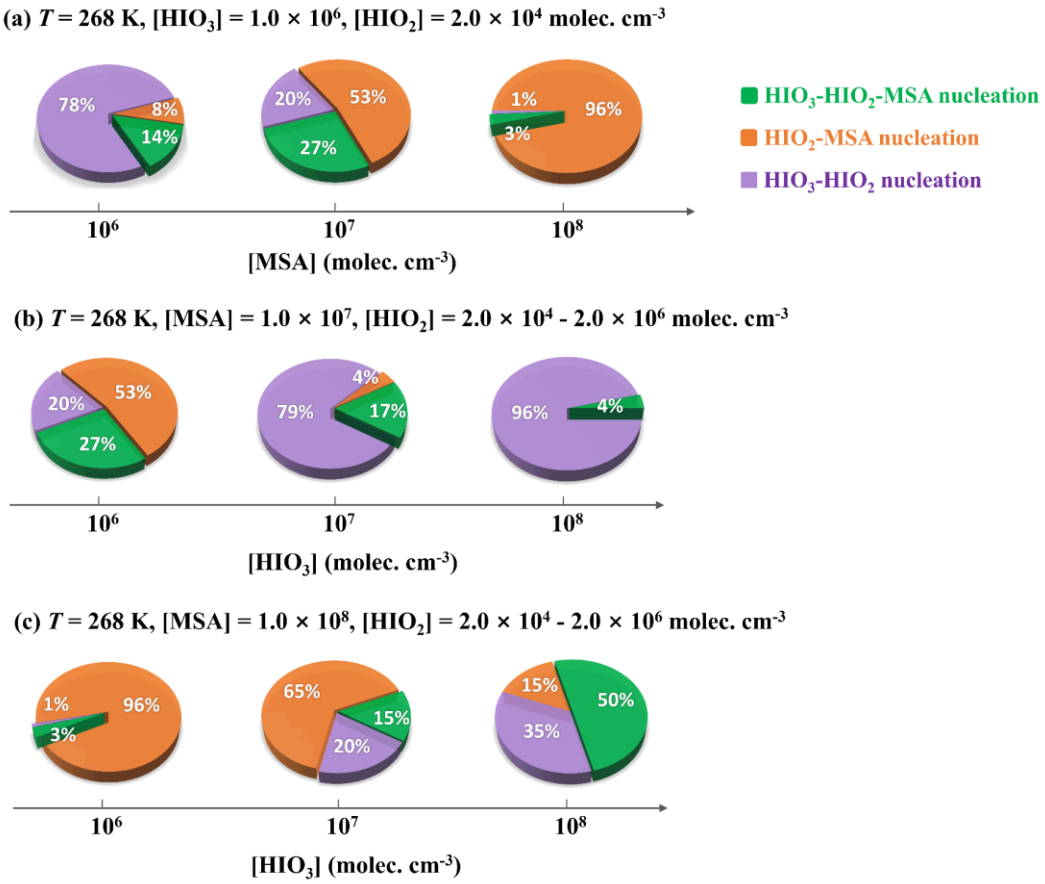

Figure S4. The branch ratio of different flux out of HIO_3-HIO_2-MSA-based system at **(a)** T = 268 K, $[HIO_3] = 1.0 \times 10^6$, $[HIO_2] = 2.0 \times 10^4$, $[MSA] = 10^6 - 10^8$ molec. cm^{-3}, **(b)** T = 268 K, $[HIO_3] = 10^6 - 10^8$, $[HIO_2] = 2.0 \times 10^4 - 2.0 \times 10^6$, $[MSA] = 1.0 \times 10^7$ molec. cm^{-3}, and **(c)** T = 268 K, $[HIO_3] = 10^6 - 10^8$, $[HIO_2] = 2.0 \times 10^4 - 2.0 \times 10^6$, $[MSA] = 1.0 \times 10^8$ molec. cm^{-3}.

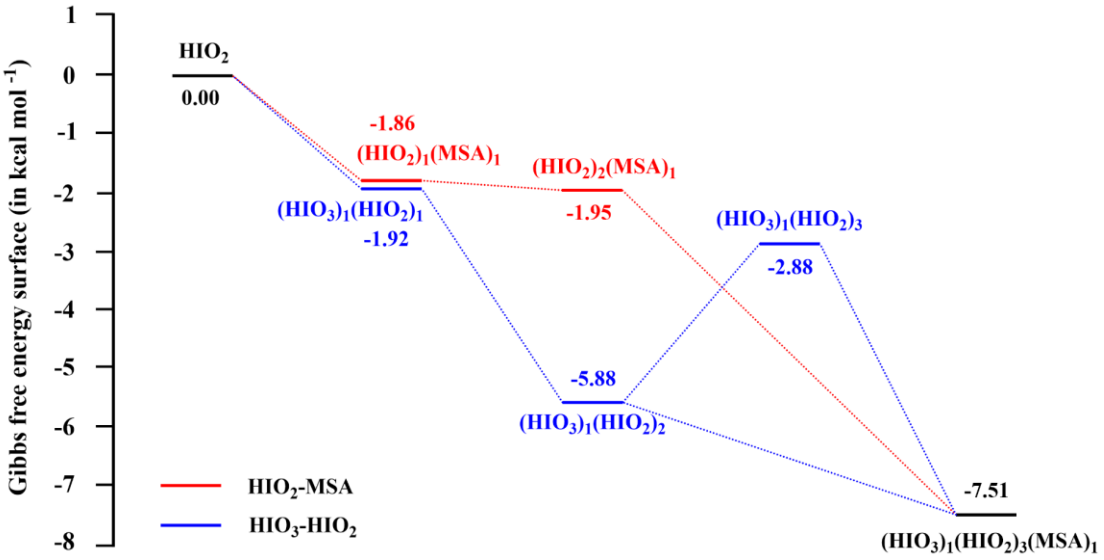

Figure S5. The Gibbs free energies of formation (ΔG, kcal mol^{-3}) of the growing clusters as a function of growth step in HIO_3-HIO_2-MSA nucleation system at T = 268 K, [HIO_3] = 1.0 × 10^6, [HIO_2] = 2.0 × 10^4, and [MSA] = 5.0 × 10^6 molec. cm^{-3}.

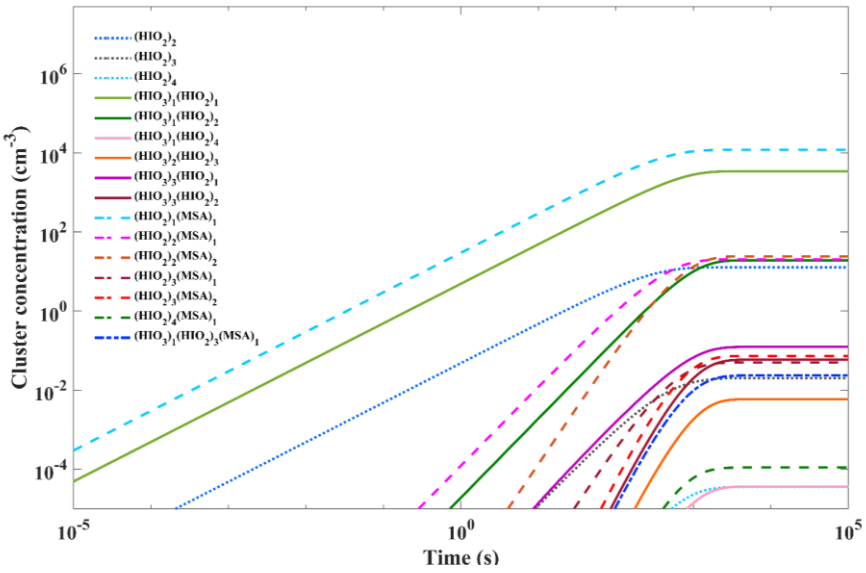

Figure S6. The concentration (molec. cm^{-3}) of stable clusters in HIO_3-HIO_2-MSA system as a function of time, at T = 278 K, CS = 2.0 × 10^{-3} s^{-1}, [HIO_3] = 10^6, [HIO_2] = 2.0 × 10^4, [MSA] = 5.0 × 10^6 molec. cm^{-3}.

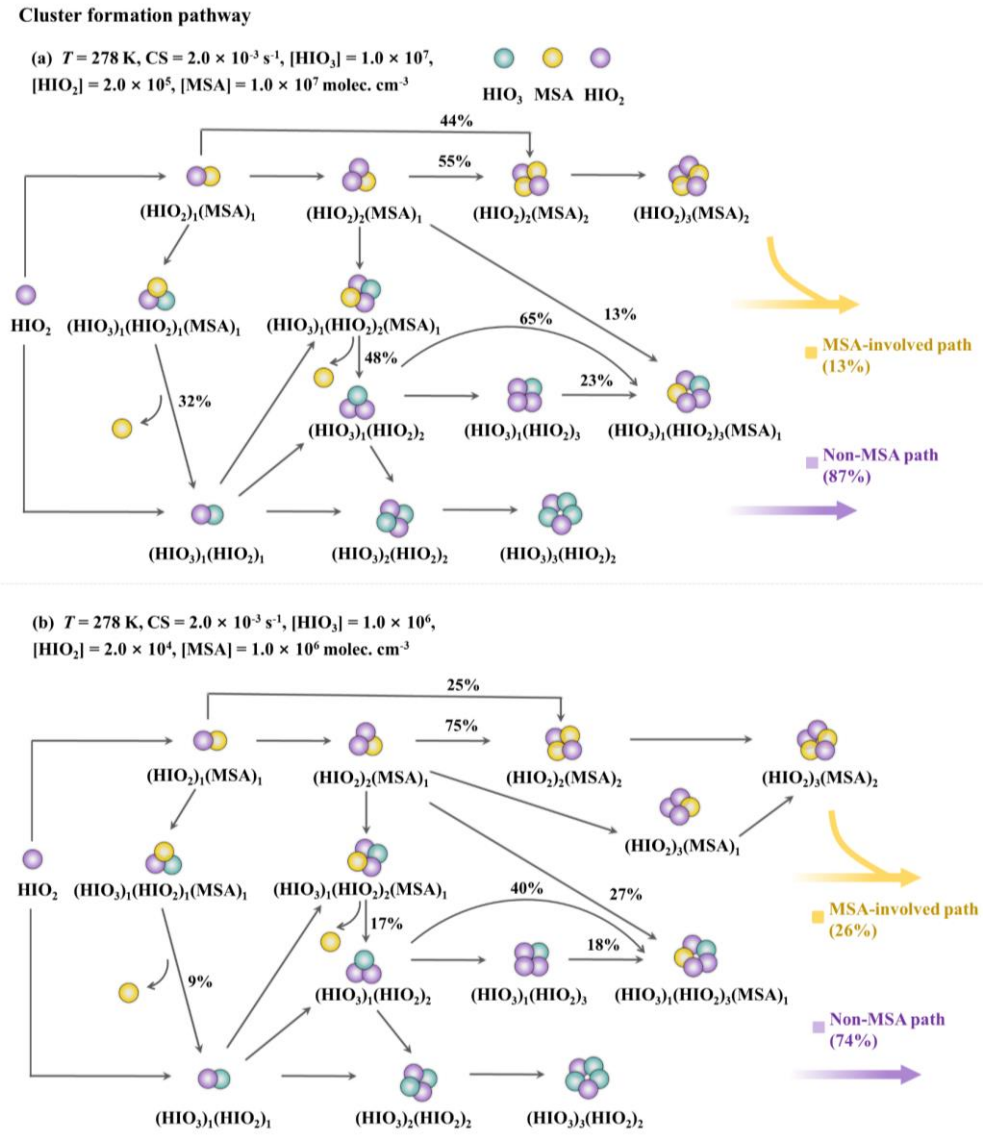

Figure S7. Main cluster growth pathway of the HIO_3-HIO_2-MSA nucleating system at T = 278K, CS = 2.0×10^{-3} s^{-1}, (a) $[HIO_3] = 1.0 \times 10^7$, $[HIO_2] = 2.0 \times 10^5$, and [MSA] = 1.0×10^7 molec. cm^{-3}, (b) $[HIO_3] = 1.0 \times 10^6$, $[HIO_2] = 2.0 \times 10^4$, and [MSA] = 1.0×10^6 molec. cm^{-3}.

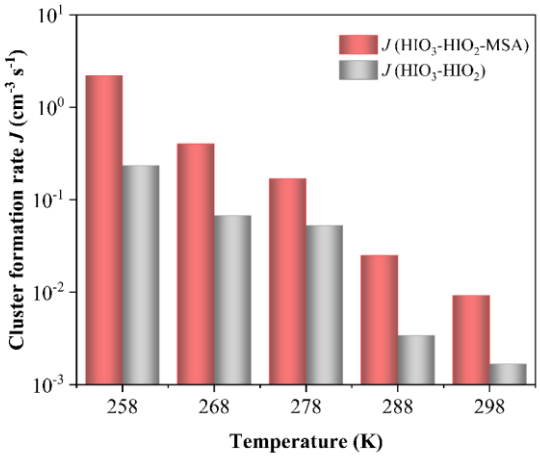

Figure S8. Simulated cluster formation rates J (cm^{-3} s^{-1}) against varying atmospheric temperatures (T = 258 – 298 K), CS = 1.0 × 10^{-2} s^{-1}, [HIO_3] = 1.0 × 10^{7}, [HIO_2] = 2.0 × 10^{5}, and [MSA] = 1.0 × 10^{7} molec. cm^{-3}.

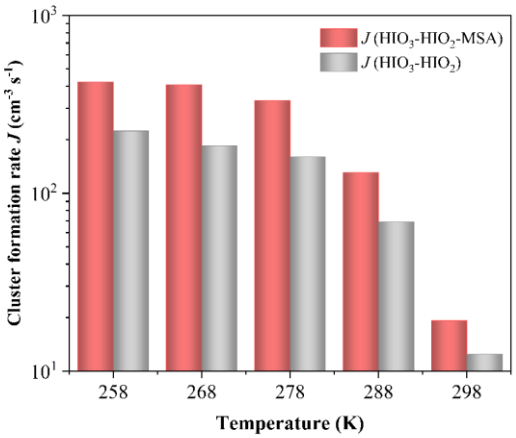

Figure S9. Simulated cluster formation rates J (cm^{-3} s^{-1}) against varying atmospheric temperatures (T = 258 – 298 K), CS = 1.0 × 10^{-4} s^{-1}, [HIO_3] = 1.0 × 10^{7}, [HIO_2] = 2.0 × 10^{5}, and [MSA] = 1.0 × 10^{7} molec. cm^{-3}.

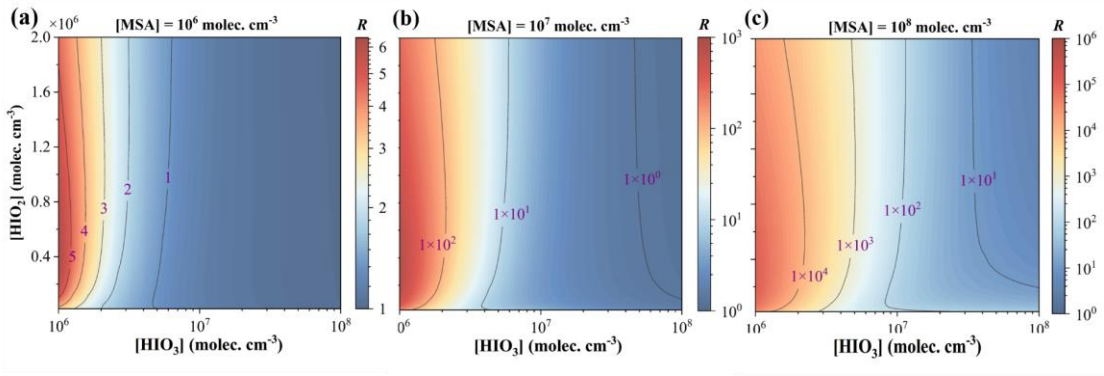

Figure S10. Enhancement strength R of MSA on cluster formation rates at varying precursor concentrations: $[HIO_3] = 10^6 – 10^8$, $[HIO_2] = 2.0 \times 10^4 – 2.0 \times 10^6$ molec. cm^{-3}, **(a)** [MSA] = 1.0×10^6 molec. cm^{-3}, **(b)** [MSA] = 1.0×10^7 molec. cm^{-3}, and **(c)** [MSA] = 1.0×10^8 molec. cm^{-3}, T = 278 K, CS = 1.0×10^{-2} s^{-1}.

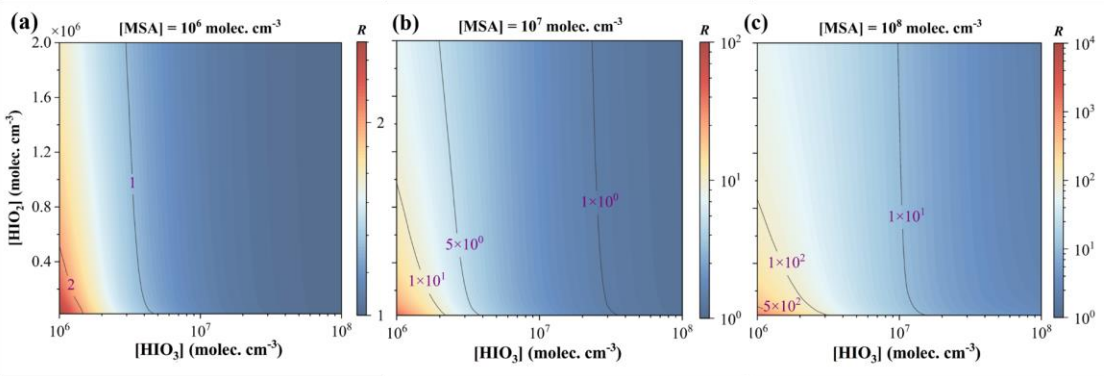

Figure S11. Enhancement strength R of MSA on cluster formation rates at varying precursor concentrations: $[HIO_3] = 10^6 – 10^8$, $[HIO_2] = 2.0 \times 10^4 – 2.0 \times 10^6$ molec. cm^{-3}, **(a)** [MSA] = 1.0×10^6 molec. cm^{-3}, **(b)** [MSA] = 1.0×10^7 molec. cm^{-3}, and **(c)** [MSA] = 1.0×10^8 molec. cm^{-3}, T = 278 K, CS = 1.0×10^{-4} s^{-1}.

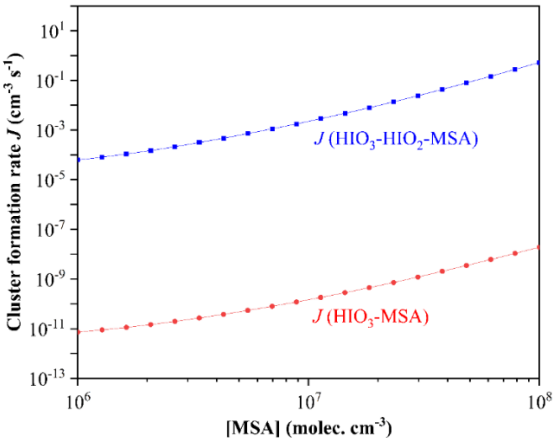

Figure S12. Simulated cluster formation rates J (cm^{-3} s^{-1}) against varying [MSA] = 10^6 – 10^7 molec. cm^{-3}, at T = 278 K, CS = 2.0 × 10^{-3} s^{-1}, [HIO_3] = 1.0 × 10^6, [HIO_2] = 2.0 × 10^4 molec. cm^{-3}.

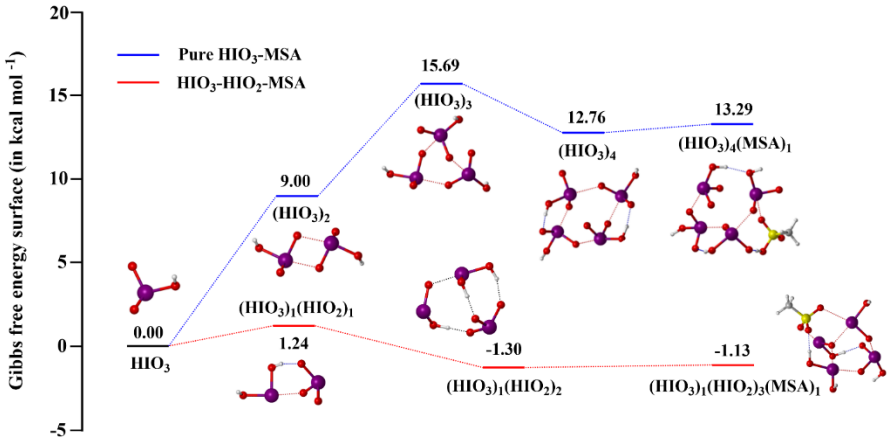

Figure S13. The Gibbs free energies of cluster formation (ΔG, kcal mol^{-1}) based on the main clustering pathway in HIO_3-MSA and HIO_3-HIO_2-MSA nucleation system at T = 278 K, CS = 2.0 × 10^{-3} s^{-1}, [HIO_3] = 1.0 × 10^6, [HIO_2] = 2.0 × 10^4 molec. cm^{-3}.

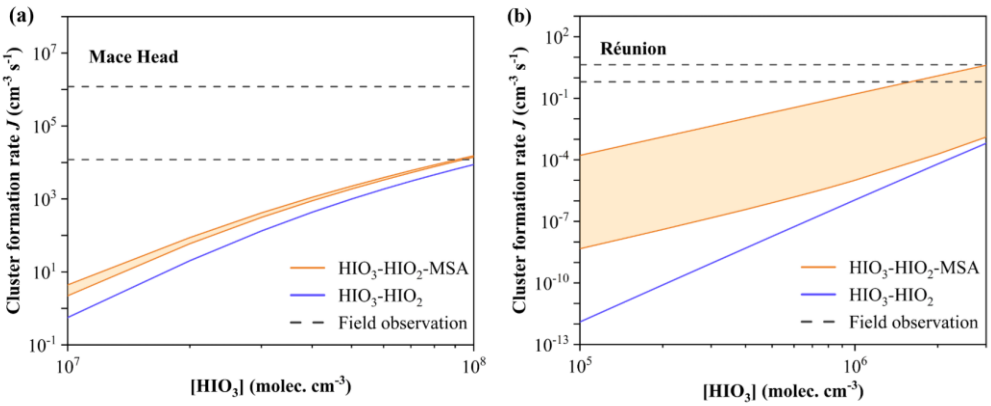

Figure S14. Comparison with the simulated cluster formation rates (J, cm^{-3} s^{-1}) and field observations at the ambient conditions of **(a)** Mace Head (T = 287 K, CS = 2.0×10^{-3} s^{-1}, $[HIO_3]$ = $10^7 - 10^8$, $[HIO_2]$ = $2.0 \times 10^5 - 2.0 \times 10^6$, and [MSA] = $10^6 - 10^7$ molec. cm^{-3}) (O'Dowd et al., 2002; Sipilä et al., 2016), (b) Réunion (T = 288 K, CS = 2.0×10^{-3} s^{-1}, $[HIO_3]$ = $10^5 - 3.0 \times 10^6$, $[HIO_2]$ = $2.0 \times 10^3 - 6.0 \times 10^4$, and [MSA] = $10^6 - 10^8$ molec. cm^{-3}). The orange area, purple line and gray area represent J(HIO_3-HIO_2-MSA), J(HIO_3-HIO_2), and J(Field observation). $[HIO_3]/[HIO_2]$ is a constant.

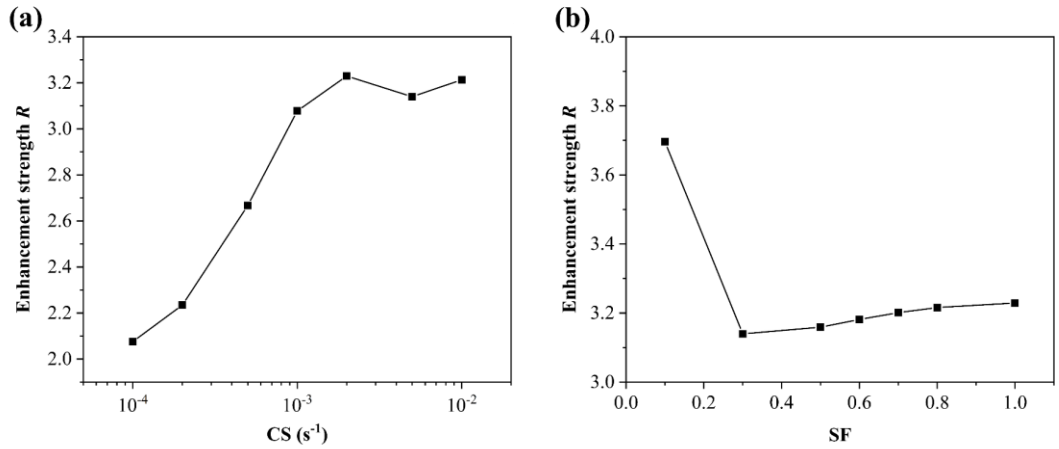

Figure S15. Variation of enhancement strength R of MSA with **(a)** condensation sink coefficient (CS) and **(b)** sticking factor (SF) for HIO_3-HIO_2-MSA system at T = 278 K, [HIO_3] = 1.0 × 10^7, [HIO_2] = 2.0 × 10^5, and [MSA] = 1.0 × 10^7 molec. cm^{-3}.

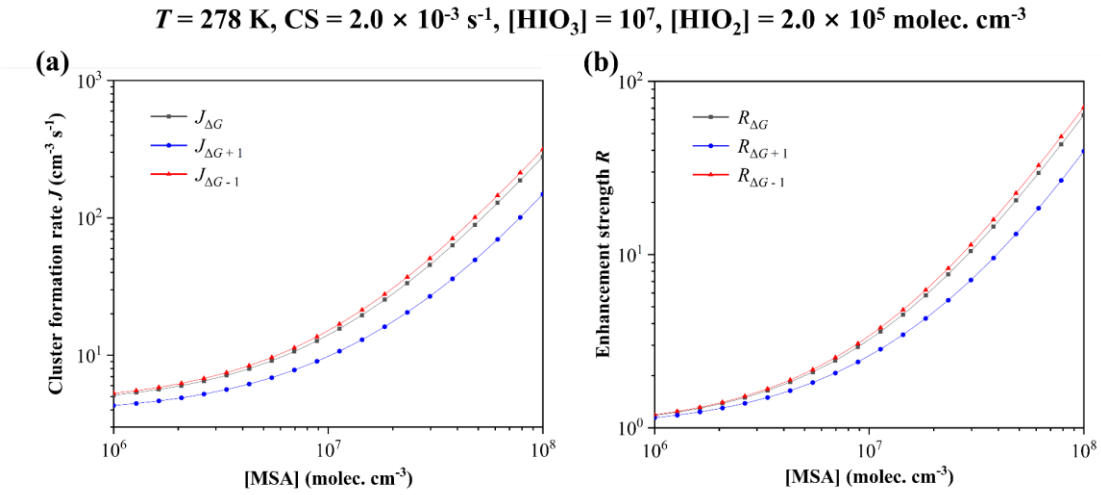

Figure S16. Cluster formation rate J **(a)** and enhancement strength R of MSA **(b)** as a function of [MSA] = 10^6 – 10^8 molec. cm^{-3}, with different Gibbs free energy of ΔG_{278K} (black line), ΔG_{278K} + 1 (blue line), ΔG_{278K} – 1 (red line), at T = 278 K, CS = 2.0 × 10^{-3} s^{-1}, [HIO_3] = 10^7, [HIO_2] = 2.0 × 10^5 molec. cm^{-3}.

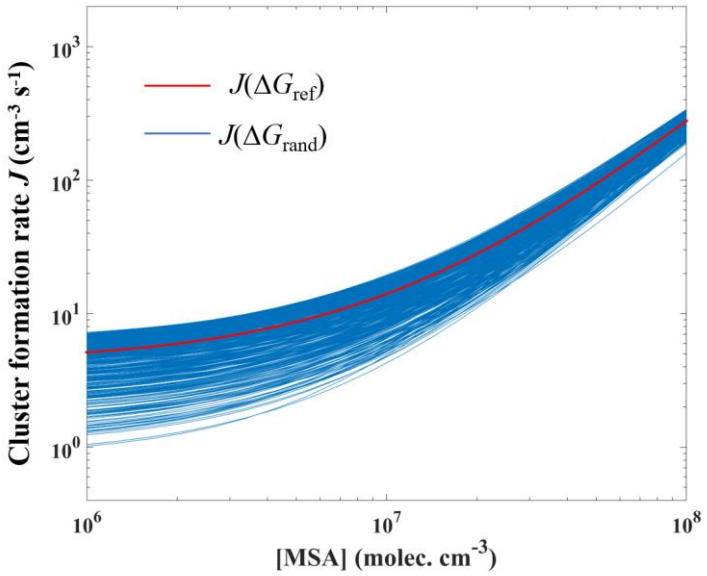

Figure S17. Cluster formation rate J (cm^{-3} s^{-1}) as a function of [MSA] = 10^6 – 10^8 molec. cm^{-3}, with different energy of ΔG_{ref} (red line, reference condition), ΔG_{rand} (blue line, randomly assigned ΔG values of all clusters within the potential bias between -1 and 1 kcal mol^{-1}), at T = 278 K, CS = 2.0 × 10^{-3} s^{-1}, [HIO_3] = 10^7, [HIO_2] = 2.0 × 10^5 molec. cm^{-3}.

Table S1. The Gibbs formation free energies ΔG_{ref} (kcal mol^{-1}) of the studied HIO_3-HIO_2-MSA clusters at the RICC2/aug-cc-pV(T+d)Z(-PP)//ωB97X-D/6-311++G(3df,3pd) + aug-cc-pVTZ-PP with ECP28MDF (for I) level of theory, p = 1 atm and T = 258, 268, 278, 288, and 298 K.

Clusters	ΔG_{ref} (kcal mol^{-1})				
	258K	268K	278K	288K	298K
$(HIO_3)_2$	-8.81	-8.45	-8.07	-7.70	-7.33
$(HIO_3)_3$	-20.04	-19.26	-18.46	-17.68	-16.89
$(HIO_3)_4$	-40.90	-39.70	-38.46	-37.26	-36.03
$(HIO_3)_5$	-59.56	-57.93	-56.26	-54.64	-52.99
$(HIO_2)_2$	-18.46	-18.05	-17.63	-17.22	-16.80
$(HIO_2)_3$	-40.76	-39.72	-39.06	-38.02	-37.38
$(HIO_2)_4$	-61.24	-59.98	-58.69	-57.45	-56.17
$(HIO_2)_5$	-79.29	-77.63	-75.92	-74.26	-72.57
$(MSA)_2$	-11.77	-11.37	-10.97	-10.57	-10.16
$(MSA)_3$	-17.64	-16.88	-16.10	-15.33	-14.55
$(HIO_3)_1(HIO_2)_1$	-18.81	-18.40	-17.99	-17.59	-17.18
$(HIO_3)_1(HIO_2)_2$	-41.44	-40.62	-39.77	-38.94	-38.10
$(HIO_3)_1(HIO_2)_3$	-57.72	-56.48	-55.20	-53.96	-52.70
$(HIO_3)_1(HIO_2)_4$	-84.22	-82.51	-80.75	-79.05	-77.30
$(HIO_3)_2(HIO_2)_1$	-32.15	-31.31	-30.46	-29.64	-28.79
$(HIO_3)_2(HIO_2)_2$	-57.64	-56.42	-55.18	-53.97	-52.73
$(HIO_3)_2(HIO_2)_3$	-81.90	-80.23	-78.52	-76.86	-75.16
$(HIO_3)_3(HIO_2)_1$	-54.15	-52.92	-51.67	-50.45	-49.21
$(HIO_3)_3(HIO_2)_2$	-76.19	-74.52	-72.80	-71.14	-69.44
$(HIO_3)_4(HIO_2)_1$	-67.80	-66.16	-64.48	-62.84	-61.18
$(HIO_3)_1(MSA)_1$	-12.09	-11.71	-11.31	-10.93	-10.54
$(HIO_3)_1(MSA)_2$	-21.32	-20.56	-19.77	-19.00	-18.22
$(HIO_3)_1(MSA)_3$	-37.28	-36.06	-34.81	-33.59	-32.34
$(HIO_3)_2(MSA)_1$	-22.59	-21.80	-21.00	-20.22	-19.42
$(HIO_3)_2(MSA)_2$	-34.34	-33.13	-31.89	-30.69	-29.46

$(HIO_3)_2(MSA)_3$	-50.31	-48.73	-47.12	-45.55	-43.94
$(HIO_3)_3(MSA)_1$	-34.53	-33.39	-32.23	-31.10	-29.94
$(HIO_3)_3(MSA)_2$	-55.17	-53.59	-51.98	-50.41	-48.81
$(HIO_3)_4(MSA)_1$	-57.49	-55.82	-54.12	-52.47	-50.78
$(HIO_2)_1(MSA)_1$	-14.25	-17.48	-17.06	-16.66	-16.25
$(HIO_2)_1(MSA)_2$	-31.38	-30.59	-29.78	-28.99	-28.18
$(HIO_2)_1(MSA)_3$	-43.04	-41.85	-40.63	-39.44	-38.22
$(HIO_2)_2(MSA)_1$	-36.95	-36.13	-35.30	-34.48	-33.65
$(HIO_2)_2(MSA)_2$	-59.94	-58.70	-57.40	-56.14	-55.25
$(HIO_2)_2(MSA)_3$	-76.23	-74.57	-72.87	-71.22	-69.52
$(HIO_2)_3(MSA)_1$	-60.98	-59.74	-58.47	-57.24	-55.98
$(HIO_2)_3(MSA)_2$	-80.96	-79.31	-77.63	-75.99	-74.31
$(HIO_2)_4(MSA)_1$	-79.57	-77.90	-76.20	-74.54	-72.84
$(HIO_3)_1(HIO_2)_1(MSA)_1$	-31.24	-30.42	-29.58	-28.77	-27.93
$(HIO_3)_1(HIO_2)_1(MSA)_2$	-47.10	-45.90	-44.67	-43.48	-42.26
$(HIO_3)_1(HIO_2)_1(MSA)_3$	-62.55	-60.92	-59.25	-57.62	-55.95
$(HIO_3)_1(HIO_2)_2(MSA)_1$	-51.78	-50.60	-49.39	-48.21	-47.01
$(HIO_3)_1(HIO_2)_2(MSA)_2$	-73.05	-71.42	-69.75	-68.13	-66.47
$(HIO_3)_1(HIO_2)_3(MSA)_1$	-78.40	-76.73	-75.02	-73.35	-71.65
$(HIO_3)_2(HIO_2)_1(MSA)_1$	-47.57	-46.33	-45.06	-43.82	-42.56
$(HIO_3)_2(HIO_2)_1(MSA)_2$	-63.94	-62.32	-60.66	-59.04	-57.39
$(HIO_3)_2(HIO_2)_2(MSA)_1$	-67.47	-65.80	-64.09	-62.43	-60.73
$(HIO_3)_3(HIO_2)_1(MSA)_1$	-67.52	-65.83	-64.10	-62.42	-60.71

Table S2. The bond type, electron density $\rho(r)$ (a.u), Laplacian electron density $\nabla^2\rho(r)$ (a.u.), energy density $H(r)$ at the corresponding bond critical points (BCPs) in the studied HIO_3-HIO_2-MSA-based clusters. The orange balls represent BCPs in the AIM theory analysis. HIO_3, HIO_2, and MSA are the shorthand for iodic acid, iodous acid and methanesulfonic acid, respectively. HB (hydrogen bond), XB (halogen bond).

Cluster	Bond	Bond type	$\rho(r)$(a.u.)	$\nabla^2\rho(r)$(a.u.)	$H(r)$ (a.u.)
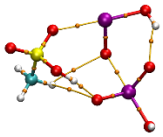 $(HIO_3)_1(HIO_2)_1(MSA)_1$	O–H···O	HB	0.0691	0.1092	-0.0248
	O–H···O	HB	0.0224	0.0823	0.0018
	O–I···O	XB	0.0786	0.1509	-0.0213
	O–I···O	XB	0.0405	0.1239	-0.0016
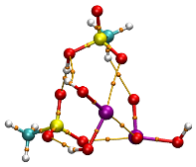 $(HIO_3)_1(HIO_2)_1(MSA)_2$	O–H···O	HB	0.0348	0.1086	-0.0021
	O–H···O	HB	0.0090	0.0310	0.0009
	O–H···O	HB	0.0582	0.1156	-0.0017
	O–I···O	XB	0.0429	0.1257	-0.0023
	O–I···O	XB	0.0476	0.1348	-0.0034
	O–I···O	XB	0.0299	0.0919	0.0003
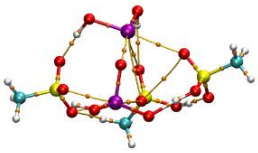 $(HIO_3)_1(HIO_2)_1(MSA)_3$	O–H···O	HB	0.0154	0.0620	0.0024
	O–H···O	HB	0.0521	0.1159	-0.0128
	O–H···O	HB	0.0495	0.1110	-0.0116
	O–H···O	HB	0.0783	0.0943	-0.0322
	O–I···O	XB	0.0114	0.0341	0.0006
	O–I···O	XB	0.0102	0.0288	0.0005
	O–I···O	XB	0.0190	0.0675	0.0019
	O–I···O	XB	0.0431	0.1244	-0.0025
	O–I···O	XB	0.0255	0.0873	0.0018
	O–I···O	XB	0.0381	0.1035	-0.0019
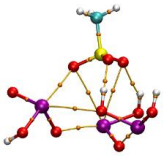	O–H···O	HB	0.0644	0.1159	-0.0206
	O–H···O	HB	0.0208	0.0803	-0.0023
	O–I···O	XB	0.0449	0.1262	-0.0031
	O–I···O	XB	0.0119	0.0358	0.0009

$(HIO_3)_1(HIO_2)_2(MSA)_1$	O–I···O	XB	0.0326	0.0952	0.0001
	O–I···O	XB	0.0116	0.0321	0.0004
	O–I···O	XB	0.0136	0.0391	0.0005
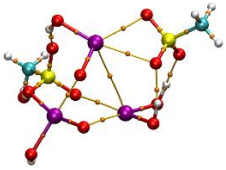 $(HIO_3)_1(HIO_2)_2(MSA)_2$	O–H···O	HB	0.0242	0.0916	0.0018
	O–H···O	HB	0.0824	0.0964	-0.0349
	O–H···O	HB	0.0383	0.1096	-0.0041
	O–H···O	HB	0.0366	0.1111	-0.0031
	O–I···O	XB	0.0927	0.1744	-0.0307
	O–I···O	XB	0.0250	0.0745	0.0003
	O–I···O	XB	0.0275	0.0784	-0.0002
	O–I···O	XB	0.0384	0.1231	-0.0006
	O–I···O	XB	0.0220	0.0724	0.0015
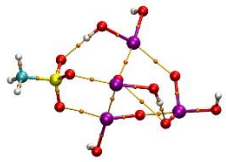 $(HIO_3)_1(HIO_2)_3(MSA)_1$	O–H···O	HB	0.0453	0.1116	-0.0085
	O–H···O	HB	0.0429	0.1091	-0.0074
	O–I···O	XB	0.0247	0.0767	0.0009
	O–I···O	XB	0.0406	0.1109	-0.0023
	O–I···O	XB	0.0499	0.1345	-0.0051
	O–I···O	XB	0.0794	0.1637	-0.0209
	O–I···O	XB	0.0648	0.1555	-0.0120
	O–I···O	XB	0.0283	0.0906	0.0011
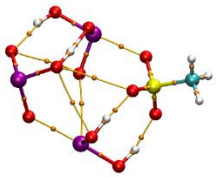 $(HIO_3)_2(HIO_2)_1(MSA)_1$	O–H···O	HB	0.0487	0.1180	-0.0103
	O–H···O	HB	0.0405	0.1131	-0.0054
	O–H···O	HB	0.0869	0.0835	-0.0394
	O–H···O	HB	0.0221	0.0793	0.0016
	O–I···O	XB	0.0386	0.1171	-0.0010
	O–I···O	XB	0.0135	0.0422	0.0012
	O–I···O	XB	0.1999	0.4607	-0.1372
	O–H···O	HB	0.0482	0.1163	-0.0104
	O–H···O	HB	0.0268	0.1079	0.0023
	O–H···O	HB	0.0627	0.1092	-0.0204

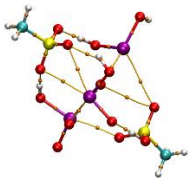 $(HIO_3)_2(HIO_2)_1(MSA)_2$	O–H···O	HB	0.0586	0.1154	-0.0170
	O–I···O	XB	0.0122	0.0376	0.0009
	O–I···O	XB	0.0712	0.1462	-0.0165
	O–I···O	XB	0.0178	0.0554	0.0007
	O–I···O	XB	0.0215	0.0710	0.0008
	O–I···O	XB	0.0248	0.0802	0.0015
	O–I···O	XB	0.0607	0.1554	-0.0097
	O–I···O	XB	0.0068	0.0205	0.0007
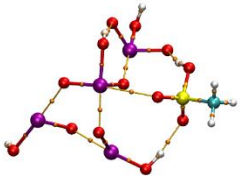 $(HIO_3)_2(HIO_2)_2(MSA)_1$	O–H···O	HB	0.0309	0.1010	-0.0010
	O–H···O	HB	0.0696	0.1038	-0.0254
	O–H···O	HB	0.0351	0.1040	-0.0029
	O–I···O	XB	0.0212	0.0675	0.0014
	O–I···O	XB	0.0911	0.1693	-0.0297
	O–I···O	XB	0.0644	0.1487	-0.0122
	O–I···O	XB	0.0548	0.1427	-0.0070
	O–I···O	XB	0.0621	0.1511	-0.0104
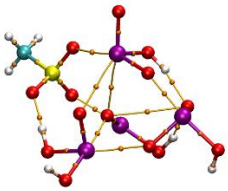 $(HIO_3)_3(HIO_2)_1(MSA)_1$	O–H···O	HB	0.0356	0.1017	-0.0032
	O–H···O	HB	0.0336	0.1016	-0.0020
	O–H···O	HB	0.0542	0.1108	-0.0147
	O–I···O	XB	0.0258	0.0780	0.0010
	O–I···O	XB	0.0756	0.1668	-0.0181
	O–I···O	XB	0.0152	0.0451	0.0008
	O–I···O	XB	0.0230	0.0709	0.0010
	O–I···O	XB	0.0566	0.1467	-0.0079
	O–I···O	XB	0.0811	0.1587	-0.0225

Table S3. Boundary conditions at 258, 268, 278, 288, and 298 K, respectively.

Temperature (K)	Boundary cluster
258 K	$(HIO_3)_6$
	$(HIO_3)_5(HIO_2)_1$
	$(HIO_3)_5(MSA)_1$
	$(HIO_3)_1(HIO_2)_5$
	$(HIO_2)_6$
	$(HIO_2)_5(MSA)_1$
	$(HIO_3)_4(MSA)_2$
	$(HIO_3)_3(MSA)_3$
	$(HIO_2)_4(MSA)_2$
	$(HIO_2)_3(MSA)_3$
	$(HIO_3)_3(HIO_2)_3$
	$(HIO_3)_2(HIO_2)_4$
	$(HIO_3)_4(HIO_2)_2$
	$(HIO_3)_3(HIO_2)_1(MSA)_2$
	$(HIO_3)_1(HIO_2)_2(MSA)_3$
	$(HIO_3)_1(HIO_2)_3(MSA)_2$
	$(HIO_3)_1(HIO_2)_4(MSA)_1$
	$(HIO_3)_2(HIO_2)_3(MSA)_1$
	$(HIO_3)_3(HIO_2)_2(MSA)_1$
268 K	$(HIO_3)_6$
	$(HIO_3)_5(MSA)_1$
	$(HIO_3)_1(HIO_2)_5$
	$(HIO_2)_5(MSA)_1$
	$(HIO_3)_2(HIO_2)_4$
	$(HIO_3)_3(HIO_2)_3$
	$(HIO_2)_4(MSA)_2$
	$(HIO_2)_3(MSA)_3$

	$(HIO_3)_4(HIO_2)_2$
	$(HIO_3)_4(MSA)_2$
	$(HIO_3)_3(MSA)_3$
	$(HIO_3)_1(HIO_2)_3(MSA)_2$
	$(HIO_3)_3(HIO_2)_2(MSA)_1$
	$(HIO_3)_3(HIO_2)_1(MSA)_2$
	$(HIO_3)_1(HIO_2)_4(MSA)_1$
	$(HIO_3)_2(HIO_2)_3(MSA)_1$
278 K	$(HIO_3)_6$
	$(HIO_3)_5(MSA)_1$
	$(HIO_3)_2(HIO_2)_4$
	$(HIO_3)_1(HIO_2)_5$
	$(HIO_3)_3(HIO_2)_3$
	$(HIO_3)_4(HIO_2)_2$
	$(HIO_3)_4(MSA)_2$
	$(HIO_3)_3(MSA)_3$
	$(HIO_2)_4(MSA)_2$
	$(HIO_2)_5(MSA)_1$
	$(HIO_2)_3(MSA)_3$
	$(HIO_3)_1(HIO_2)_3(MSA)_2$
	$(HIO_3)_3(HIO_2)_1(MSA)_2$
	$(HIO_3)_3(HIO_2)_2(MSA)_1$
	$(HIO_3)_2(HIO_2)_3(MSA)_1$
	$(HIO_3)_1(HIO_2)_4(MSA)_1$
288 K	$(HIO_3)_2(HIO_2)_4$
	$(HIO_3)_1(HIO_2)_5$
	$(HIO_3)_3(HIO_2)_3$
	$(HIO_3)_4(MSA)_2$
	$(HIO_3)_3(MSA)_3$
	$(HIO_2)_3(MSA)_3$

	$(HIO_3)_1(HIO_2)_4(MSA)_1$
	$(HIO_3)_2(HIO_2)_3(MSA)_1$
	$(HIO_3)_1(HIO_2)_3(MSA)_2$
298 K	$(HIO_3)_2(HIO_2)_4$
	$(HIO_3)_1(HIO_2)_5$
	$(HIO_3)_3(HIO_2)_3$
	$(HIO_3)_4(MSA)_2$
	$(HIO_3)_3(MSA)_3$
	$(HIO_2)_3(MSA)_3$
	$(HIO_3)_1(HIO_2)_4(MSA)_1$
	$(HIO_3)_2(HIO_2)_3(MSA)_1$

Table S4. The ratios of HIO_3 monomer collision frequencies versus total evaporation rate coefficients ($\beta C/\Sigma\gamma$) at T = 258, 268, 278, 288, and 298 K. β is the rate coefficient of cluster collision with HIO_3 monomer, and C is the concentration of HIO_3 monomer (1.0×10^6 molecules cm^{-3}).

Clusters	$\beta C/\Sigma\gamma$				
	258K	268K	278K	288K	298K
$(HIO_3)_2$	2.19×10^{-6}	6.08×10^{-7}	1.79×10^{-7}	5.86×10^{-8}	2.10×10^{-8}
$(HIO_3)_3$	1.25×10^{-4}	2.61×10^{-5}	6.09×10^{-6}	1.60×10^{-6}	4.55×10^{-7}
$(HIO_3)_4$	1.77×10^{4}	1.83×10^{3}	2.15×10^{2}	3.05×10^{1}	4.84×10^{0}
$(HIO_3)_5$	2.40×10^{2}	2.86×10^{1}	3.97×10^{0}	6.46×10^{-1}	1.22×10^{-1}
$(HIO_2)_2$	3.27×10^{2}	4.10×10^{1}	5.87×10^{0}	9.81×10^{-1}	1.85×10^{-1}
$(HIO_2)_3$	2.97×10^{5}	1.86×10^{4}	2.89×10^{3}	2.59×10^{2}	3.77×10^{1}
$(HIO_2)_4$	8.40×10^{3}	1.30×10^{1}	1.10×10^{2}	2.33×10^{1}	3.80×10^{0}
$(HIO_2)_5$	7.24×10^{1}	9.54×10^{0}	1.41×10^{0}	2.37×10^{-1}	6.16×10^{-2}
$(MSA)_2$	5.82×10^{-4}	1.21×10^{-4}	2.83×10^{-5}	7.31×10^{-6}	2.07×10^{-6}
$(MSA)_3$	2.88×10^{-9}	9.92×10^{-10}	3.57×10^{-10}	1.40×10^{-10}	5.87×10^{-11}
$(HIO_3)_1(HIO_2)_1$	1.62×10^{2}	1.98×10^{1}	2.83×10^{0}	4.70×10^{-1}	8.68×10^{-2}
$(HIO_3)_1(HIO_2)_2$	3.75×10^{5}	3.45×10^{4}	3.59×10^{3}	4.45×10^{2}	6.44×10^{1}
$(HIO_3)_1(HIO_2)_3$	1.83×10^{0}	2.82×10^{-1}	4.27×10^{-2}	8.71×10^{-3}	1.83×10^{-3}
$(HIO_3)_1(HIO_2)_4$	1.10×10^{6}	9.20×10^{4}	8.90×10^{3}	1.03×10^{3}	1.40×10^{2}
$(HIO_3)_2(HIO_2)_1$	1.86×10^{0}	1.33×10^{-3}	2.61×10^{-4}	5.92×10^{-5}	1.46×10^{-5}
$(HIO_3)_2(HIO_2)_2$	2.01×10^{0}	3.03×10^{-1}	5.34×10^{-2}	1.08×10^{-2}	2.36×10^{-3}
$(HIO_3)_2(HIO_2)_3$	6.12×10^{6}	4.78×10^{5}	4.41×10^{4}	4.93×10^{3}	6.34×10^{2}
$(HIO_3)_3(HIO_2)_1$	1.66×10^{5}	1.67×10^{4}	1.95×10^{3}	2.65×10^{2}	4.19×10^{1}
$(HIO_3)_3(HIO_2)_2$	1.94×10^{2}	2.24×10^{1}	2.87×10^{0}	4.47×10^{-1}	8.00×10^{-2}
$(HIO_3)_4(HIO_2)_1$	1.36×10^{-2}	2.19×10^{-3}	4.73×10^{-4}	1.06×10^{-4}	2.67×10^{-5}
$(HIO_3)_1(MSA)_1$	2.88×10^{-4}	6.08×10^{-5}	1.39×10^{-5}	3.63×10^{-6}	1.04×10^{-6}
$(HIO_3)_1(MSA)_2$	1.39×10^{-6}	3.63×10^{-7}	1.01×10^{-7}	3.14×10^{-8}	1.05×10^{-8}
$(HIO_3)_1(MSA)_3$	9.73×10^{-1}	1.33×10^{-1}	2.11×10^{-2}	3.87×10^{-3}	7.83×10^{-4}
$(HIO_3)_2(MSA)_1$	2.91×10^{-5}	6.50×10^{-6}	1.65×10^{-6}	4.63×10^{-7}	4.24×10^{-10}
$(HIO_3)_2(MSA)_2$	2.50×10^{-4}	4.98×10^{-5}	1.07×10^{-5}	2.67×10^{-6}	7.33×10^{-6}

$(HIO_3)_2(MSA)_3$	4.02×10^{-3}	8.22×10^{-4}	1.89×10^{-4}	4.88×10^{-5}	1.40×10^{-5}
$(HIO_3)_3(MSA)_1$	4.86×10^{-4}	1.09×10^{-4}	2.70×10^{-5}	7.48×10^{-6}	1.12×10^{-4}
$(HIO_3)_3(MSA)_2$	5.72×10^{3}	6.03×10^{2}	7.36×10^{1}	1.05×10^{1}	1.71×10^{0}
$(HIO_3)_4(MSA)_1$	3.27×10^{0}	4.20×10^{-1}	6.46×10^{-2}	1.13×10^{-2}	2.22×10^{-3}
$(HIO_2)_1(MSA)_1$	1.96×10^{-2}	3.11×10^{0}	4.63×10^{-1}	8.17×10^{-2}	1.59×10^{-2}
$(HIO_2)_1(MSA)_2$	1.00×10^{1}	1.59×10^{-3}	3.36×10^{-4}	7.91×10^{-5}	2.06×10^{-5}
$(HIO_2)_1(MSA)_3$	2.26×10^{-4}	4.75×10^{-5}	1.10×10^{-5}	2.86×10^{-6}	8.15×10^{-7}
$(HIO_2)_2(MSA)_1$	1.45×10^{2}	1.41×10^{1}	2.03×10^{0}	3.35×10^{-1}	6.25×10^{-2}
$(HIO_2)_2(MSA)_2$	8.96×10^{5}	7.94×10^{4}	7.66×10^{3}	9.17×10^{2}	1.23×10^{2}
$(HIO_2)_2(MSA)_3$	1.84×10^{0}	2.68×10^{-1}	4.56×10^{-2}	9.13×10^{-3}	1.82×10^{-3}
$(HIO_2)_3(MSA)_1$	4.06×10^{3}	6.65×10^{2}	5.91×10^{1}	1.30×10^{1}	2.25×10^{0}
$(HIO_2)_3(MSA)_2$	2.23×10^{3}	2.49×10^{2}	3.27×10^{1}	4.95×10^{0}	1.11×10^{0}
$(HIO_2)_4(MSA)_1$	6.70×10^{1}	8.33×10^{0}	1.20×10^{0}	1.97×10^{-1}	7.22×10^{-2}
$(HIO_3)_1(HIO_2)_1(MSA)_1$	1.05×10^{-3}	1.79×10^{-4}	3.76×10^{-5}	9.10×10^{-6}	2.39×10^{-6}
$(HIO_3)_1(HIO_2)_1(MSA)_2$	3.94×10^{-1}	6.18×10^{-2}	1.09×10^{-2}	2.22×10^{-3}	5.08×10^{-4}
$(HIO_3)_1(HIO_2)_1(MSA)_3$	3.61×10^{-1}	5.43×10^{-2}	9.21×10^{-3}	1.77×10^{-3}	3.80×10^{-4}
$(HIO_3)_1(HIO_2)_2(MSA)_1$	1.73×10^{-5}	4.30×10^{-6}	1.19×10^{-6}	3.64×10^{-7}	1.21×10^{-7}
$(HIO_3)_1(HIO_2)_2(MSA)_2$	4.77×10^{-3}	9.18×10^{-4}	2.06×10^{-4}	5.25×10^{-5}	1.46×10^{-5}
$(HIO_3)_1(HIO_2)_3(MSA)_1$	2.13×10^{1}	2.77×10^{0}	4.12×10^{-1}	6.98×10^{-2}	1.34×10^{-2}
$(HIO_3)_2(HIO_2)_1(MSA)_1$	3.06×10^{-1}	4.83×10^{-2}	8.40×10^{-3}	1.65×10^{-3}	3.75×10^{-4}
$(HIO_3)_2(HIO_2)_1(MSA)_2$	1.63×10^{0}	2.46×10^{-1}	4.16×10^{-2}	8.05×10^{-3}	1.74×10^{-3}
$(HIO_3)_2(HIO_2)_2(MSA)_1$	6.17×10^{-6}	1.35×10^{-6}	3.20×10^{-7}	8.53×10^{-8}	2.59×10^{-8}
$(HIO_3)_3(HIO_2)_1(MSA)_1$	6.16×10^{-3}	1.02×10^{-3}	1.86×10^{-4}	3.94×10^{-5}	9.29×10^{-6}

Table S5. The evaporation rate coefficients (γ, s^{-1}) for all evaporation pathways of clusters at 268 K.

Evaporation pathways	Evaporation rate coefficients (γ, s^{-1})
$(HIO_3)_2 \rightarrow HIO_3 + HIO_3$	4.28×10^{2}
$(HIO_3)_3 \rightarrow (HIO_3)_2 + HIO_3$	1.09×10^{1}
$(HIO_3)_4 \rightarrow (HIO_3)_3 + HIO_3$	1.67×10^{-7}
$(HIO_3)_5 \rightarrow (HIO_3)_4 + HIO_3$	1.14×10^{-5}
$(HIO_2)_2 \rightarrow HIO_2 + HIO_2$	6.19×10^{-6}
$(HIO_2)_3 \rightarrow (HIO_2)_2 + HIO_2$	1.48×10^{-8}
$(HIO_2)_4 \rightarrow (HIO_2)_3 + HIO_2$	2.28×10^{-7}
$(HIO_2)_5 \rightarrow (HIO_2)_4 + HIO_2$	3.31×10^{-5}
$(MSA)_2 \rightarrow MSA + MSA$	2.55×10^{0}
$(MSA)_3 \rightarrow (MSA)_2 + MSA$	3.34×10^{5}
$(HIO_3)_1(HIO_2)_1 \rightarrow HIO_3 + HIO_2$	1.30×10^{-5}
$(HIO_3)_1(HIO_2)_2 \rightarrow HIO_3 + (HIO_2)_2$	2.73×10^{-9}
$(HIO_3)_1(HIO_2)_2 \rightarrow (HIO_3)_1(HIO_2)_1 + HIO_2$	5.36×10^{-9}
$(HIO_3)_1(HIO_2)_3 \rightarrow HIO_3 + (HIO_2)_3$	1.62×10^{-4}
$(HIO_3)_1(HIO_2)_3 \rightarrow (HIO_3)_1(HIO_2)_2 + HIO_2$	8.96×10^{-4}
$(HIO_3)_1(HIO_2)_4 \rightarrow HIO_3 + (HIO_2)_4$	3.44×10^{-9}
$(HIO_3)_1(HIO_2)_4 \rightarrow (HIO_3)_1(HIO_2)_3 + HIO_2$	4.89×10^{-12}
$(HIO_3)_2(HIO_2)_1 \rightarrow HIO_3 + (HIO_3)_1(HIO_2)_1$	2.10×10^{-1}
$(HIO_3)_2(HIO_2)_1 \rightarrow (HIO_3)_2 + HIO_2$	1.63×10^{-9}
$(HIO_3)_2(HIO_2)_2 \rightarrow HIO_3 + (HIO_3)_1(HIO_2)_2$	9.98×10^{-4}
$(HIO_3)_2(HIO_2)_2 \rightarrow (HIO_3)_2(HIO_2)_1 + HIO_2$	2.57×10^{-11}
$(HIO_3)_2(HIO_2)_3 \rightarrow HIO_3 + (HIO_3)_1(HIO_2)_3$	3.50×10^{-10}
$(HIO_3)_2(HIO_2)_3 \rightarrow (HIO_3)_2(HIO_2)_2 + HIO_2$	3.21×10^{-10}
$(HIO_3)_3(HIO_2)_1 \rightarrow HIO_3 + (HIO_3)_2(HIO_2)_1$	1.83×10^{-8}
$(HIO_3)_3(HIO_2)_1 \rightarrow (HIO_3)_3 + HIO_2$	2.78×10^{-18}
$(HIO_3)_3(HIO_2)_2 \rightarrow HIO_3 + (HIO_3)_2(HIO_2)_2$	1.44×10^{-5}
$(HIO_3)_3(HIO_2)_2 \rightarrow (HIO_3)_3(HIO_2)_1 + HIO_2$	2.05×10^{-8}

$(HIO_3)_4(HIO_2)_1 \rightarrow HIO_3 + (HIO_3)_3(HIO_2)_1$	1.34×10^{-1}
$(HIO_3)_4(HIO_2)_1 \rightarrow (HIO_3)_4 + HIO_2$	2.24×10^{-12}
$(HIO_3)_1(MSA)_1 \rightarrow HIO_3 + MSA$	2.30×10^{0}
$(HIO_3)_1(MSA)_2 \rightarrow HIO_3 + (MSA)_2$	2.71×10^{2}
$(HIO_3)_1(MSA)_2 \rightarrow (HIO_3)_1(MSA)_1 + MSA$	5.86×10^{2}
$(HIO_3)_1(MSA)_3 \rightarrow HIO_3 + (MSA)_3$	2.07×10^{-6}
$(HIO_3)_1(MSA)_3 \rightarrow (HIO_3)_1(MSA)_2 + MSA$	2.50×10^{-3}
$(HIO_3)_2(MSA)_1 \rightarrow HIO_3 + (HIO_3)_1(MSA)_1$	4.54×10^{1}
$(HIO_3)_2(MSA)_1 \rightarrow (HIO_3)_2 + MSA$	1.19×10^{-1}
$(HIO_3)_2(MSA)_2 \rightarrow HIO_3 + (HIO_3)_1(MSA)_2$	4.79×10^{-1}
$(HIO_3)_2(MSA)_2 \rightarrow (HIO_3)_2(MSA)_1 + MSA$	6.04×10^{0}
$(HIO_3)_2(MSA)_3 \rightarrow HIO_3 + (HIO_3)_1(MSA)_3$	4.25×10^{-1}
$(HIO_3)_2(MSA)_3 \rightarrow (HIO_3)_2(MSA)_2 + MSA$	2.20×10^{-3}
$(HIO_3)_3(MSA)_1 \rightarrow HIO_3 + (HIO_3)_2(MSA)_1$	2.87×10^{0}
$(HIO_3)_3(MSA)_1 \rightarrow (HIO_3)_3 + MSA$	3.05×10^{-2}
$(HIO_3)_3(MSA)_2 \rightarrow HIO_3 + (HIO_3)_2(MSA)_2$	1.84×10^{-7}
$(HIO_3)_3(MSA)_2 \rightarrow (HIO_3)_3(MSA)_1 + MSA$	3.84×10^{-7}
$(HIO_3)_4(MSA)_1 \rightarrow HIO_3 + (HIO_3)_3(MSA)_1$	4.44×10^{-9}
$(HIO_3)_4(MSA)_1 \rightarrow (HIO_3)_4 + MSA$	7.93×10^{-4}
$(HIO_2)_1(MSA)_1 \rightarrow HIO_2 + MSA$	4.45×10^{-5}
$(HIO_2)_1(MSA)_2 \rightarrow HIO_2 + (MSA)_2$	1.78×10^{-6}
$(HIO_2)_1(MSA)_2 \rightarrow (HIO_2)_1(MSA)_1 + MSA$	1.94×10^{-1}
$(HIO_2)_1(MSA)_3 \rightarrow HIO_2 + (MSA)_3$	3.94×10^{-11}
$(HIO_2)_1(MSA)_3 \rightarrow (HIO_2)_1(MSA)_2 + MSA$	7.09×10^{0}
$(HIO_3)_2(MSA)_1 \rightarrow HIO_2 + (HIO_2)_1(MSA)_1$	4.68×10^{-6}
$(HIO_2)_2(MSA)_1 \rightarrow (HIO_2)_2 + MSA$	1.60×10^{-5}
$(HIO_2)_2(MSA)_2 \rightarrow HIO_2 + (HIO_2)_1(MSA)_2$	1.01×10^{-13}
$(HIO_2)_2(MSA)_2 \rightarrow (HIO_2)_2(MSA)_1 + MSA$	4.04×10^{-9}
$(HIO_2)_2(MSA)_3 \rightarrow HIO_2 + (HIO_2)_1(MSA)_3$	1.93×10^{-17}
$(HIO_2)_2(MSA)_3 \rightarrow (HIO_2)_2(MSA)_2 + MSA$	1.31×10^{-3}

$(HIO_2)_3(MSA)_1 \rightarrow HIO_2 + (HIO_2)_2(MSA)_1$	4.46×10^{-10}
$(HIO_2)_3(MSA)_1 \rightarrow (HIO_2)_3 + MSA$	4.63×10^{-7}
$(HIO_2)_3(MSA)_2 \rightarrow HIO_2 + (HIO_2)_2(MSA)_2$	1.38×10^{-7}
$(HIO_2)_3(MSA)_2 \rightarrow (HIO_2)_3(MSA)_1 + MSA$	1.21×10^{-6}
$(HIO_2)_4(MSA)_1 \rightarrow HIO_2 + (HIO_2)_3(MSA)_1$	1.32×10^{-5}
$(HIO_2)_4(MSA)_1 \rightarrow (HIO_2)_4 + MSA$	2.60×10^{-5}
$(HIO_3)_1(HIO_2)_1(MSA)_1 \rightarrow HIO_3 + (HIO_2)_1\ (MSA)_1$	2.13×10^{-1}
$(HIO_3)_1(HIO_2)_1(MSA)_1 \rightarrow HIO_2 + (HIO_3)_1(MSA)_1$	4.23×10^{-6}
$(HIO_3)_1(HIO_2)_1(MSA)_1 \rightarrow MSA + (HIO_3)_1(HIO_2)_1$	1.42×10^{0}
$(HIO_3)_1(HIO_2)_1(MSA)_2 \rightarrow HIO_3 + (HIO_2)_1(MSA)_2$	2.76×10^{-3}
$(HIO_3)_1(HIO_2)_1(MSA)_2 \rightarrow HIO_2 + (HIO_3)_1(MSA)_2$	1.85×10^{-11}
$(HIO_3)_1(HIO_2)_1(MSA)_2 \rightarrow MSA + (HIO_3)_1(HIO_2)_1(MSA)_1$	2.46×10^{-3}
$(HIO_3)_1(HIO_2)_1(MSA)_3 \rightarrow HIO_3 + (HIO_2)_1(MSA)_3$	2.59×10^{-6}
$(HIO_3)_1(HIO_2)_1(MSA)_3 \rightarrow HIO_2 + (HIO_3)_1(MSA)_3$	4.91×10^{-11}
$(HIO_3)_1(HIO_2)_1(MSA)_3 \rightarrow MSA + (HIO_3)_1(HIO_2)_1(MSA)_2$	6.50×10^{-3}
$(HIO_3)_1(HIO_2)_2(MSA)_1 \rightarrow HIO_3 + (HIO_2)_2(MSA)_1$	1.26×10^{-2}
$(HIO_3)_1(HIO_2)_2(MSA)_1 \rightarrow HIO_2 + (HIO_3)_1(HIO_2)_1(MSA)_1$	2.81×10^{-7}
$(HIO_3)_1(HIO_2)_2(MSA)_1 \rightarrow MSA + (HIO_3)_1(HIO_2)_2$	7.23×10^{1}
$(HIO_3)_1(HIO_2)_2(MSA)_2 \rightarrow HIO_3 + (HIO_2)_2(MSA)_2$	3.72×10^{-1}
$(HIO_3)_1(HIO_2)_2(MSA)_2 \rightarrow HIO_2 + (HIO_3)_1(HIO_2)_1(MSA)_2$	1.38×10^{-11}
$(HIO_3)_1(HIO_2)_2(MSA)_2 \rightarrow MSA + (HIO_3)_1(HIO_2)_2(MSA)_1$	1.17×10^{-7}
$(HIO_3)_1(HIO_2)_3(MSA)_1 \rightarrow HIO_3 + (HIO_2)_3(MSA)_1$	1.18×10^{-4}
$(HIO_3)_1(HIO_2)_3(MSA)_1 \rightarrow HIO_2 + (HIO_3)_1(HIO_2)_2(MSA)_1$	4.23×10^{-12}
$(HIO_3)_1(HIO_2)_3(MSA)_1 \rightarrow MSA + (HIO_3)_1(HIO_2)_3$	3.30×10^{-7}
$(HIO_3)_2(HIO_2)_1(MSA)_1 \rightarrow HIO_3 + (HIO_3)_1(HIO_2)_1(MSA)_1$	8.50×10^{-4}
$(HIO_3)_2(HIO_2)_1(MSA)_1 \rightarrow HIO_2 + (HIO_3)_2(MSA)_1$	8.08×10^{-11}
$(HIO_3)_2(HIO_2)_1(MSA)_1 \rightarrow MSA + (HIO_3)_2(HIO_2)_1$	5.64×10^{-3}
$(HIO_3)_2(HIO_2)_1(MSA)_2 \rightarrow HIO_3 + (HIO_3)_1(HIO_2)_1(MSA)_2$	3.60×10^{-4}
$(HIO_3)_2(HIO_2)_1(MSA)_2 \rightarrow HIO_2 + (HIO_3)_2(MSA)_2$	1.41×10^{-14}
$(HIO_3)_2(HIO_2)_1(MSA)_2 \rightarrow MSA + (HIO_3)_2(HIO_2)_1(MSA)_1$	1.03×10^{-3}

$(HIO_3)_2(HIO_2)_2(MSA)_1 \rightarrow HIO_3 + (HIO_3)_1(HIO_2)_2(MSA)_1$	3.43×10^{-3}
$(HIO_3)_2(HIO_2)_2(MSA)_1 \rightarrow HIO_2 + (HIO_3)_2(HIO_2)_1(MSA)_1$	1.15×10^{-6}
$(HIO_3)_2(HIO_2)_2(MSA)_1 \rightarrow MSA + (HIO_3)_2(HIO_2)_2$	2.45×10^{2}
$(HIO_3)_3(HIO_2)_1(MSA)_1 \rightarrow HIO_3 + (HIO_3)_2(HIO_2)_1(MSA)_1$	1.08×10^{-6}
$(HIO_3)_3(HIO_2)_1(MSA)_1 \rightarrow HIO_2 + (HIO_3)_3(MSA)_1$	3.08×10^{-17}
$(HIO_3)_3(HIO_2)_1(MSA)_1 \rightarrow MSA + (HIO_3)_3(HIO_2)_1$	3.27×10^{-1}

Table S6. The evaporation rate coefficients (γ, s^{-1}) for all evaporation pathways of clusters at 278 K.

Evaporation pathways	Evaporation rate coefficients (γ, s^{-1})
$(HIO_3)_2 \rightarrow HIO_3 + HIO_3$	1.48×10^{3}
$(HIO_3)_3 \rightarrow (HIO_3)_2 + HIO_3$	4.76×10^{1}
$(HIO_3)_4 \rightarrow (HIO_3)_3 + HIO_3$	1.45×10^{-6}
$(HIO_3)_5 \rightarrow (HIO_3)_4 + HIO_3$	8.37×10^{-5}
$(HIO_2)_2 \rightarrow HIO_2 + HIO_2$	4.40×10^{-5}
$(HIO_2)_3 \rightarrow (HIO_2)_2 + HIO_2$	9.68×10^{-8}
$(HIO_2)_4 \rightarrow (HIO_2)_3 + HIO_2$	2.75×10^{-6}
$(HIO_2)_5 \rightarrow (HIO_2)_4 + HIO_2$	2.29×10^{-4}
$(MSA)_2 \rightarrow MSA + MSA$	1.11×10^{1}
$(MSA)_3 \rightarrow (MSA)_2 + MSA$	9.46×10^{5}
$(HIO_3)_1(HIO_2)_1 \rightarrow HIO_3 + HIO_2$	9.30×10^{-5}
$(HIO_3)_1(HIO_2)_2 \rightarrow HIO_3 + (HIO_2)_2$	2.68×10^{-8}
$(HIO_3)_1(HIO_2)_2 \rightarrow (HIO_3)_1(HIO_2)_1 + HIO_2$	5.24×10^{-8}
$(HIO_3)_1(HIO_2)_3 \rightarrow HIO_3 + (HIO_2)_3$	1.52×10^{-3}
$(HIO_3)_1(HIO_2)_3 \rightarrow (HIO_3)_1(HIO_2)_2 + HIO_2$	5.59×10^{-3}
$(HIO_3)_1(HIO_2)_4 \rightarrow HIO_3 + (HIO_2)_4$	3.62×10^{-8}
$(HIO_3)_1(HIO_2)_4 \rightarrow (HIO_3)_1(HIO_2)_3 + HIO_2$	6.64×10^{-11}
$(HIO_3)_2(HIO_2)_1 \rightarrow HIO_3 + (HIO_3)_1(HIO_2)_1$	1.09×10^{0}
$(HIO_3)_2(HIO_2)_1 \rightarrow (HIO_3)_2 + HIO_2$	1.75×10^{-8}
$(HIO_3)_2(HIO_2)_2 \rightarrow HIO_3 + (HIO_3)_1(HIO_2)_2$	5.77×10^{-3}
$(HIO_3)_2(HIO_2)_2 \rightarrow (HIO_3)_2(HIO_2)_1 + HIO_2$	2.79×10^{-10}
$(HIO_3)_2(HIO_2)_3 \rightarrow HIO_3 + (HIO_3)_1(HIO_2)_3$	3.73×10^{-9}
$(HIO_3)_2(HIO_2)_3 \rightarrow (HIO_3)_2(HIO_2)_2 + HIO_2$	3.68×10^{-9}
$(HIO_3)_3(HIO_2)_1 \rightarrow HIO_3 + (HIO_3)_2(HIO_2)_1$	1.59×10^{-7}
$(HIO_3)_3(HIO_2)_1 \rightarrow (HIO_3)_3 + HIO_2$	6.01×10^{-17}
$(HIO_3)_3(HIO_2)_2 \rightarrow HIO_3 + (HIO_3)_2(HIO_2)_2$	1.14×10^{-4}
$(HIO_3)_3(HIO_2)_2 \rightarrow (HIO_3)_3(HIO_2)_1 + HIO_2$	2.03×10^{-7}

$(HIO_3)_4(HIO_2)_1 \rightarrow HIO_3 + (HIO_3)_3(HIO_2)_1$	6.98×10^{-1}
$(HIO_3)_4(HIO_2)_1 \rightarrow (HIO_3)_4 + HIO_2$	2.92×10^{-11}
$(HIO_3)_1(MSA)_1 \rightarrow HIO_3 + MSA$	1.03×10^{1}
$(HIO_3)_1(MSA)_2 \rightarrow HIO_3 + (MSA)_2$	1.00×10^{3}
$(HIO_3)_1(MSA)_2 \rightarrow (HIO_3)_1(MSA)_1 + MSA$	2.12×10^{3}
$(HIO_3)_1(MSA)_3 \rightarrow HIO_3 + (MSA)_3$	1.74×10^{-5}
$(HIO_3)_1(MSA)_3 \rightarrow (HIO_3)_1(MSA)_2 + MSA$	1.61×10^{-2}
$(HIO_3)_2(MSA)_1 \rightarrow HIO_3 + (HIO_3)_1(MSA)_1$	1.82×10^{2}
$(HIO_3)_2(MSA)_1 \rightarrow (HIO_3)_2 + MSA$	6.13×10^{-1}
$(HIO_3)_2(MSA)_2 \rightarrow HIO_3 + (HIO_3)_1(MSA)_2$	2.48×10^{0}
$(HIO_3)_2(MSA)_2 \rightarrow (HIO_3)_2(MSA)_1 + MSA$	2.83×10^{1}
$(HIO_3)_2(MSA)_3 \rightarrow HIO_3 + (HIO_3)_1(MSA)_3$	1.88×10^{0}
$(HIO_3)_2(MSA)_3 \rightarrow (HIO_3)_2(MSA)_2 + MSA$	1.21×10^{-2}
$(HIO_3)_3(MSA)_1 \rightarrow HIO_3 + (HIO_3)_2(MSA)_1$	1.18×10^{1}
$(HIO_3)_3(MSA)_1 \rightarrow (HIO_3)_3 + MSA$	1.49×10^{-1}
$(HIO_3)_3(MSA)_2 \rightarrow HIO_3 + (HIO_3)_2(MSA)_2$	1.40×10^{-6}
$(HIO_3)_3(MSA)_2 \rightarrow (HIO_3)_3(MSA)_1 + MSA$	3.33×10^{-6}
$(HIO_3)_4(MSA)_1 \rightarrow HIO_3 + (HIO_3)_3(MSA)_1$	5.28×10^{-8}
$(HIO_3)_4(MSA)_1 \rightarrow (HIO_3)_4 + MSA$	5.32×10^{-3}
$(HIO_2)_1(MSA)_1 \rightarrow HIO_2 + MSA$	3.05×10^{-4}
$(HIO_2)_1(MSA)_2 \rightarrow HIO_2 + (MSA)_2$	1.35×10^{-5}
$(HIO_2)_1(MSA)_2 \rightarrow (HIO_2)_1(MSA)_1 + MSA$	9.35×10^{-1}
$(HIO_2)_1(MSA)_3 \rightarrow HIO_2 + (MSA)_3$	4.63×10^{-10}
$(HIO_2)_1(MSA)_3 \rightarrow (HIO_2)_1(MSA)_2 + MSA$	3.13×10^{1}
$(HIO_3)_2(MSA)_1 \rightarrow HIO_2 + (HIO_2)_1(MSA)_1$	3.40×10^{-5}
$(HIO_2)_2(MSA)_1 \rightarrow (HIO_2)_2 + MSA$	1.12×10^{-4}
$(HIO_2)_2(MSA)_2 \rightarrow HIO_2 + (HIO_2)_1(MSA)_2$	1.61×10^{-12}
$(HIO_2)_2(MSA)_2 \rightarrow (HIO_2)_2(MSA)_1 + MSA$	4.26×10^{-8}
$(HIO_2)_2(MSA)_3 \rightarrow HIO_2 + (HIO_2)_1(MSA)_3$	4.12×10^{-16}
$(HIO_2)_2(MSA)_3 \rightarrow (HIO_2)_2(MSA)_2 + MSA$	7.73×10^{-3}

$(HIO_2)_3(MSA)_1 \rightarrow HIO_2 + (HIO_2)_2(MSA)_1$	4.78×10^{-9}
$(HIO_2)_3(MSA)_1 \rightarrow (HIO_2)_3 + MSA$	5.30×10^{-6}
$(HIO_2)_3(MSA)_2 \rightarrow HIO_2 + (HIO_2)_2(MSA)_2$	1.08×10^{-6}
$(HIO_2)_3(MSA)_2 \rightarrow (HIO_2)_3(MSA)_1 + MSA$	9.38×10^{-6}
$(HIO_2)_4(MSA)_1 \rightarrow HIO_2 + (HIO_2)_3(MSA)_1$	9.62×10^{-5}
$(HIO_2)_4(MSA)_1 \rightarrow (HIO_2)_4 + MSA$	1.80×10^{-4}
$(HIO_3)_1(HIO_2)_1(MSA)_1 \rightarrow HIO_3 + (HIO_2)_1\ (MSA)_1$	1.07×10^{0}
$(HIO_3)_1(HIO_2)_1(MSA)_1 \rightarrow HIO_2 + (HIO_3)_1(MSA)_1$	3.26×10^{-5}
$(HIO_3)_1(HIO_2)_1(MSA)_1 \rightarrow MSA + (HIO_3)_1(HIO_2)_1$	6.86×10^{0}
$(HIO_3)_1(HIO_2)_1(MSA)_2 \rightarrow HIO_3 + (HIO_2)_1(MSA)_2$	1.63×10^{-2}
$(HIO_3)_1(HIO_2)_1(MSA)_2 \rightarrow HIO_2 + (HIO_3)_1(MSA)_2$	2.23×10^{-10}
$(HIO_3)_1(HIO_2)_1(MSA)_2 \rightarrow MSA + (HIO_3)_1(HIO_2)_1(MSA)_1$	1.39×10^{-2}
$(HIO_3)_1(HIO_2)_1(MSA)_3 \rightarrow HIO_3 + (HIO_2)_1(MSA)_3$	2.08×10^{-5}
$(HIO_3)_1(HIO_2)_1(MSA)_3 \rightarrow HIO_2 + (HIO_3)_1(MSA)_3$	5.52×10^{-10}
$(HIO_3)_1(HIO_2)_1(MSA)_3 \rightarrow MSA + (HIO_3)_1(HIO_2)_1(MSA)_2$	3.91×10^{-2}
$(HIO_3)_1(HIO_2)_2(MSA)_1 \rightarrow HIO_3 + (HIO_2)_2(MSA)_1$	6.55×10^{-2}
$(HIO_3)_1(HIO_2)_2(MSA)_1 \rightarrow HIO_2 + (HIO_3)_1(HIO_2)_1(MSA)_1$	2.11×10^{-6}
$(HIO_3)_1(HIO_2)_2(MSA)_1 \rightarrow MSA + (HIO_3)_1(HIO_2)_2$	2.67×10^{2}
$(HIO_3)_1(HIO_2)_2(MSA)_2 \rightarrow HIO_3 + (HIO_2)_2(MSA)_2$	1.68×10^{0}
$(HIO_3)_1(HIO_2)_2(MSA)_2 \rightarrow HIO_2 + (HIO_3)_1(HIO_2)_1(MSA)_2$	1.68×10^{-10}
$(HIO_3)_1(HIO_2)_2(MSA)_2 \rightarrow MSA + (HIO_3)_1(HIO_2)_2(MSA)_1$	1.08×10^{-6}
$(HIO_3)_1(HIO_2)_3(MSA)_1 \rightarrow HIO_3 + (HIO_2)_3(MSA)_1$	8.08×10^{-4}
$(HIO_3)_1(HIO_2)_3(MSA)_1 \rightarrow HIO_2 + (HIO_3)_1(HIO_2)_2(MSA)_1$	5.99×10^{-11}
$(HIO_3)_1(HIO_2)_3(MSA)_1 \rightarrow MSA + (HIO_3)_1(HIO_2)_3$	2.77×10^{-6}
$(HIO_3)_2(HIO_2)_1(MSA)_1 \rightarrow HIO_3 + (HIO_3)_1(HIO_2)_1(MSA)_1$	5.32×10^{-3}
$(HIO_3)_2(HIO_2)_1(MSA)_1 \rightarrow HIO_2 + (HIO_3)_2(MSA)_1$	9.73×10^{-10}
$(HIO_3)_2(HIO_2)_1(MSA)_1 \rightarrow MSA + (HIO_3)_2(HIO_2)_1$	3.26×10^{-2}
$(HIO_3)_2(HIO_2)_1(MSA)_2 \rightarrow HIO_3 + (HIO_3)_1(HIO_2)_1(MSA)_2$	2.34×10^{-3}
$(HIO_3)_2(HIO_2)_1(MSA)_2 \rightarrow HIO_2 + (HIO_3)_2(MSA)_2$	2.12×10^{-13}
$(HIO_3)_2(HIO_2)_1(MSA)_2 \rightarrow MSA + (HIO_3)_2(HIO_2)_1(MSA)_1$	6.02×10^{-3}

$(HIO_3)_2(HIO_2)_2(MSA)_1 \rightarrow HIO_3 + (HIO_3)_1(HIO_2)_2(MSA)_1$	2.33×10^{-2}
$(HIO_3)_2(HIO_2)_2(MSA)_1 \rightarrow HIO_2 + (HIO_3)_2(HIO_2)_1(MSA)_1$	9.31×10^{-6}
$(HIO_3)_2(HIO_2)_2(MSA)_1 \rightarrow MSA + (HIO_3)_2(HIO_2)_2$	1.06×10^{3}
$(HIO_3)_3(HIO_2)_1(MSA)_1 \rightarrow HIO_3 + (HIO_3)_2(HIO_2)_1(MSA)_1$	9.06×10^{-6}
$(HIO_3)_3(HIO_2)_1(MSA)_1 \rightarrow HIO_2 + (HIO_3)_3(MSA)_1$	7.06×10^{-16}
$(HIO_3)_3(HIO_2)_1(MSA)_1 \rightarrow MSA + (HIO_3)_3(HIO_2)_1$	1.83×10^{0}

Table S7. The total evaporation rate coefficients ($\Sigma\gamma$, s^{-1}) of clusters calculated at 278 K.

Cluster	$\Sigma\gamma$ (s^{-1})
$(HIO_3)_2$	1.48×10^{3}
$(HIO_3)_3$	4.76×10^{1}
$(HIO_3)_4$	1.45×10^{-6}
$(HIO_3)_5$	8.37×10^{-5}
$(HIO_2)_2$	4.40×10^{-5}
$(HIO_2)_3$	9.68×10^{-8}
$(HIO_2)_4$	2.75×10^{-6}
$(HIO_2)_5$	2.29×10^{-4}
$(MSA)_2$	1.11×10^{1}
$(MSA)_3$	9.46×10^{5}
$(HIO_3)_1(HIO_2)_1$	9.30×10^{-5}
$(HIO_3)_1(HIO_2)_2$	7.92×10^{-8}
$(HIO_3)_1(HIO_2)_3$	7.11×10^{-3}
$(HIO_3)_1(HIO_2)_4$	3.63×10^{-8}
$(HIO_3)_2(HIO_2)_1$	1.09×10^{0}
$(HIO_3)_2(HIO_2)_2$	5.77×10^{-3}
$(HIO_3)_2(HIO_2)_3$	7.41×10^{-9}
$(HIO_3)_3(HIO_2)_1$	1.59×10^{-7}
$(HIO_3)_3(HIO_2)_2$	1.15×10^{-4}
$(HIO_3)_4(HIO_2)_1$	6.98×10^{-1}
$(HIO_3)_1(MSA)_1$	2.06×10^{1}
$(HIO_3)_1(MSA)_2$	3.12×10^{3}
$(HIO_3)_1(MSA)_3$	1.61×10^{-2}
$(HIO_3)_2(MSA)_1$	1.82×10^{2}
$(HIO_3)_2(MSA)_2$	3.08×10^{1}
$(HIO_3)_2(MSA)_3$	1.90×10^{0}
$(HIO_3)_3(MSA)_1$	1.20×10^{1}
$(HIO_3)_3(MSA)_2$	4.74×10^{-6}

$(HIO_3)_4(MSA)_1$	5.32×10^{-3}
$(HIO_2)_1(MSA)_1$	6.09×10^{-4}
$(HIO_2)_1(MSA)_2$	9.35×10^{-1}
$(HIO_2)_1(MSA)_3$	3.13×10^{1}
$(HIO_3)_2(MSA)_1$	1.46×10^{-4}
$(HIO_2)_2(MSA)_2$	4.26×10^{-8}
$(HIO_2)_2(MSA)_3$	7.73×10^{-3}
$(HIO_2)_3(MSA)_1$	5.30×10^{-6}
$(HIO_2)_3(MSA)_2$	1.05×10^{-5}
$(HIO_2)_4(MSA)_1$	2.76×10^{-4}
$(HIO_3)_1(HIO_2)_1(MSA)_1$	7.93×10^{0}
$(HIO_3)_1(HIO_2)_1(MSA)_2$	3.03×10^{-2}
$(HIO_3)_1(HIO_2)_1(MSA)_3$	3.91×10^{-2}
$(HIO_3)_1(HIO_2)_2(MSA)_1$	2.68×10^{2}
$(HIO_3)_1(HIO_2)_2(MSA)_2$	1.68×10^{0}
$(HIO_3)_1(HIO_2)_3(MSA)_1$	8.11×10^{-4}
$(HIO_3)_2(HIO_2)_1(MSA)_1$	3.80×10^{-2}
$(HIO_3)_2(HIO_2)_1(MSA)_2$	8.35×10^{-3}
$(HIO_3)_2(HIO_2)_2(MSA)_1$	1.06×10^{3}
$(HIO_3)_3(HIO_2)_1(MSA)_1$	1.83×10^{0}

Table S8. Cluster formation rate J of HIO_3-HIO_2-MSA system under different Gibbs free energy (ΔG_{278K}, ΔG_{278K} + 1, ΔG_{278K} - 1) at T = 278 K, CS = 2.0×10^{-3} s^{-1}, [HIO_3] = 10^7, [HIO_2] = 2.0×10^5, [MSA] = 10^6 – 10^8 molec. cm^{-3}.

[MSA]	$J_{\Delta G}$	$J_{\Delta G-1}$	$J_{\Delta G+1}$
1.00×10^6	5.13×10^0	4.31×10^0	5.29×10^0
1.27×10^6	5.35×10^0	4.46×10^0	5.53×10^0
1.62×10^6	5.64×10^0	4.65×10^0	5.84×10^0
2.07×10^6	6.01×10^0	4.90×10^0	6.25×10^0
2.64×10^6	6.50×10^0	5.22×10^0	6.78×10^0
3.36×10^6	7.14×10^0	5.63×10^0	7.47×10^0
4.28×10^6	7.99×10^0	6.17×10^0	8.40×10^0
5.46×10^6	9.12×10^0	6.87×10^0	9.64×10^0
6.95×10^6	1.06×10^1	7.80×10^0	1.13×10^1
8.86×10^6	1.27×10^1	9.04×10^0	1.36×10^1
1.13×10^7	1.56×10^1	1.07×10^1	1.68×10^1
1.44×10^7	1.96×10^1	1.30×10^1	2.14×10^1
1.83×10^7	2.53×10^1	1.61×10^1	2.78×10^1
2.34×10^7	3.35×10^1	2.05×10^1	3.71×10^1
2.98×10^7	4.55×10^1	2.68×10^1	5.07×10^1
3.79×10^7	6.31×10^1	3.60×10^1	7.08×10^1
4.83×10^7	8.93×10^1	4.95×10^1	1.01×10^2
6.16×10^7	1.29×10^2	6.98×10^1	1.46×10^2
7.85×10^7	1.88×10^2	1.01×10^2	2.13×10^2
1.00×10^8	2.78×10^2	1.49×10^2	3.15×10^2

Table S9. Cartesian coordinates of all clusters in the present study at the ωB97X-D/6-311++G(3df,3pd) + aug-cc-pVTZ-PP with ECP28MDF (for I) level of theory.

$(HIO_3)_1(HIO_2)_1(MSA)_1$:

Atoms	X	Y	Z
I	-1.877771	-0.752509	0.232491
O	-0.595483	-1.823796	-0.441557
O	-2.129309	0.529646	-0.990503
O	-3.347446	-1.887376	-0.363133
H	-3.316493	-2.009666	-1.318151
I	0.538518	1.786822	-0.007683
O	-0.280369	0.538764	1.127138
O	-0.982028	2.977162	-0.164915
H	-1.650294	2.452812	-0.639218
C	2.381400	-2.002110	1.293918
H	1.349560	-1.779093	1.553529
H	3.055380	-1.690334	2.087356
H	2.513617	-3.055293	1.064019
S	2.803335	-1.068186	-0.135331
O	4.109943	-1.391523	-0.576780
O	2.557737	0.329273	0.190156
O	1.799377	-1.531930	-1.201161
H	0.827546	-1.555140	-0.894535

$(HIO_3)_1(HIO_2)_1(MSA)_2$:

Atoms	X	Y	Z
I	2.409779	0.774129	-0.040206
O	1.385502	0.576253	1.430168
O	1.373911	1.601378	-1.214087
O	3.392857	2.316656	0.600986
H	2.789785	3.054133	0.751657
I	-0.952983	-0.240914	1.639934
O	-0.192173	-1.842568	2.353516
O	-2.791548	-0.834672	1.828123
H	-3.101196	-1.123232	0.961065
C	-1.635090	1.941809	-2.395478
H	-1.580410	3.023401	-2.301298
H	-2.078867	1.657620	-3.345129
H	-0.648400	1.503914	-2.254014
S	-2.689253	1.381700	-1.107970
O	-4.018312	1.835580	-1.303795
O	-2.052011	1.693605	0.151464

O	-2.703961	-0.170078	-1.294340
H	-1.806699	-0.574127	-1.495560
C	1.026057	-3.296909	-2.467723
H	1.757678	-3.951230	-2.002419
H	1.462361	-2.757735	-3.303648
H	0.154792	-3.862035	-2.787581
S	0.493560	-2.124785	-1.266745
O	-0.450874	-1.245829	-1.942264
O	1.721432	-1.408995	-0.868687
O	-0.082162	-2.871797	-0.166188
H	-0.035276	-2.407404	1.566781

$(HIO_3)_1(HIO_2)_1(MSA)_3$:

Atoms	X	Y	Z
I	-0.704502	1.880683	-0.087693
O	-0.262147	0.962564	-1.568210
O	0.769896	2.880001	0.140275
O	-1.718617	3.284402	-0.904918
H	-2.597548	2.909382	-1.066314
I	0.237573	-1.482650	-1.552860
O	-1.493460	-1.862291	-2.239184
O	0.793149	-3.313365	-1.239210
H	0.691830	-3.449932	-0.285722
C	-5.131422	-0.202325	0.675597
H	-5.602298	-0.293691	-0.299047
H	-5.397670	0.738529	1.148982
H	-5.404847	-1.040327	1.311180
S	-3.380752	-0.239309	0.457515
O	-2.769644	-0.081762	1.758671
O	-3.073136	0.902025	-0.429969
O	-3.081940	-1.512628	-0.184028
H	-2.145756	-1.747538	-1.495636
C	-0.352326	-1.151292	3.638131
H	-0.161837	-2.038803	4.234685
H	-1.363857	-1.142807	3.232807
H	-0.156843	-0.242376	4.199162
S	0.707021	-1.179657	2.247421
O	0.510522	0.019993	1.474837
O	0.561143	-2.434754	1.578032
O	2.110374	-1.088098	2.898449
H	2.710461	-0.516583	2.343792
C	5.133324	0.642192	-0.731776
H	5.048734	0.835176	-1.797054

H	5.572150	-0.335132	-0.549498
H	5.703289	1.421137	-0.234095
S	3.517878	0.610806	-0.048159
O	3.642807	0.423119	1.378359
O	2.734434	-0.371353	-0.743488
O	3.070689	2.029833	-0.374786
H	2.095029	2.304867	-0.152704

$(HIO_3)_1(HIO_2)_2(MSA)_1$:

Atoms	X	Y	Z
I	2.348350	-0.769952	-0.370994
O	1.654492	-0.933432	1.291176
O	3.963063	-0.109532	-0.099351
O	2.813854	-2.636535	-0.606809
H	3.520811	-2.864712	0.009545
I	-2.435446	-1.030080	-0.532754
O	-0.675580	-1.017821	-1.293881
O	-3.255475	-1.247275	-2.322592
H	-3.259906	-0.405511	-2.787043
I	-0.311703	0.399257	2.003701
O	-1.453783	-0.979816	1.421811
O	-1.672202	1.741859	2.352406
H	-1.643425	2.304136	1.558194
C	0.742195	3.687612	-2.070912
H	1.452733	3.361092	-2.824708
H	1.213050	4.370788	-1.369626
H	-0.127171	4.148493	-2.531313
S	0.197366	2.274013	-1.170936
O	-0.746074	2.744114	-0.175752
O	1.404151	1.671612	-0.591398
O	-0.416216	1.381600	-2.162983
H	-0.560623	-0.101299	-1.693138

$(HIO_3)_1(HIO_2)_2(MSA)_2$:

Atoms	X	Y	Z
I	-2.274708	-1.314077	-1.069938
O	-1.280980	0.083594	-1.611998
O	-2.834872	-0.822265	0.570168
O	-3.863092	-0.664896	-2.016261
H	-3.926249	0.294889	-1.977898
I	0.632696	-1.618253	1.095082

O	-0.580722	-2.309479	-0.180893
O	-0.456420	-1.721741	2.682021
H	-0.891987	-0.855016	2.762242
I	0.688431	1.614509	-1.302574
O	2.141989	2.852309	-1.109255
O	1.534733	0.503037	-2.608748
H	2.035517	-0.157807	-2.078329
C	-2.210521	3.345329	2.878658
H	-2.770544	4.077303	2.303823
H	-1.320249	3.795666	3.309752
H	-2.828191	2.892116	3.648119
S	-1.664285	2.084478	1.787508
O	-1.022339	1.045238	2.543856
O	-0.886171	2.707518	0.750861
O	-2.999114	1.580531	1.225491
H	-2.947752	0.587627	0.928655
C	5.145879	-1.203340	0.025882
H	5.462625	-1.041750	-1.000725
H	5.004780	-2.261776	0.225378
H	5.862700	-0.773971	0.720608
S	3.604091	-0.383395	0.266973
O	3.190244	-0.626641	1.636474
O	2.649949	-1.030216	-0.671988
O	3.827983	1.010367	-0.061212
H	2.840580	2.359109	-0.624881

$(HIO_3)_1(HIO_2)_3(MSA)_1$:

Atoms	X	Y	Z
I	3.100541	-0.494953	0.054224
O	2.179606	-1.070771	1.483798
O	2.472547	1.147459	-0.315090
O	4.647763	0.187051	1.046983
H	4.402718	0.972847	1.546784
I	0.062420	2.172851	-0.950176
O	-1.809613	2.599934	-0.820501
O	0.419481	3.698110	-2.140759
H	0.228934	3.455910	-3.050887
I	-1.082332	0.306963	2.092020
O	-0.525627	0.313681	0.284389
O	0.668997	0.672503	2.819187
H	1.295934	-0.000699	2.454745
I	-0.185243	-1.901950	-0.896517
O	1.558417	-1.340313	-1.301383

O	0.003276	-3.716490	-1.607974
H	-0.125092	-3.696140	-2.560272
C	-5.285320	-0.812393	-0.216000
H	-5.786708	0.143010	-0.091180
H	-5.534282	-1.491748	0.594069
H	-5.532742	-1.254333	-1.177365
S	-3.545561	-0.530966	-0.191771
O	-2.903926	-1.828621	-0.308546
O	-3.290245	0.092168	1.128168
O	-3.248350	0.375639	-1.288410
H	-2.341954	1.803875	-1.066678

$(HIO_3)_2(HIO_2)_1(MSA)_1$:

Atoms	X	Y	Z
I	-2.773171	-0.569794	0.577742
O	-3.115255	0.810216	-0.492635
O	-1.860841	-1.790462	-0.379870
O	-1.500766	0.059435	1.789981
H	-1.001840	0.929412	1.478961
I	0.168997	2.377382	-0.567292
O	-0.382966	2.188189	1.138075
O	0.041412	0.752066	-1.270487
O	-1.481935	3.081061	-1.270734
H	-2.168376	2.402925	-1.129338
I	0.590524	-2.309932	-0.694268
O	0.649959	-2.383007	1.206637
O	2.421517	-2.794143	-1.001080
H	2.934821	-1.967440	-0.840170
C	4.280227	0.941448	1.692637
H	3.934820	1.617441	2.469557
H	5.024361	1.422211	1.063883
H	4.676566	0.026750	2.125015
S	2.901359	0.510132	0.682594
O	3.401261	-0.377603	-0.351589
O	2.430470	1.796956	0.137610
O	1.915552	-0.104451	1.559334
H	1.072665	-1.523873	1.475161

$(HIO_3)_2(HIO_2)_1(MSA)_2$:

Atoms	X	Y	Z
I	1.093782	-1.924547	-1.130100
O	0.788916	-2.106659	0.671617
O	2.174892	-3.259322	-1.508651
O	-0.532941	-2.693983	-1.742588
H	-1.290898	-2.408139	-1.167747
I	-0.260065	-0.431970	1.808869
O	-0.040004	0.373751	0.174644
O	1.270762	-0.102861	2.655767
O	-1.103125	1.122009	2.601535
H	-2.038169	1.063428	2.341988
I	-0.816885	2.364153	-0.728820
O	-1.345194	1.183577	-2.120771
O	-1.576969	3.955428	-1.584113
H	-0.997674	4.261083	-2.287831
C	-4.943314	-1.579588	0.211887
H	-5.685012	-0.789147	0.284178
H	-4.933230	-2.183615	1.114711
H	-5.126029	-2.197329	-0.662966
S	-3.359337	-0.831759	0.033773
O	-2.382689	-1.918557	-0.030515
O	-3.139910	-0.018473	1.224822
O	-3.424062	-0.045957	-1.192370
H	-2.173130	0.707090	-1.814150
C	5.156706	1.385513	-0.097012
H	5.394987	2.292011	0.451764
H	5.308485	1.532078	-1.163093
H	5.735971	0.540665	0.262797
S	3.451272	1.032543	0.125257
O	3.167615	-0.230034	-0.510885
O	2.670833	2.156196	-0.287817
O	3.422602	0.866210	1.656187
H	2.555533	0.478486	2.004433

$(HIO_3)_2(HIO_2)_2(MSA)_1$:

Atoms	X	Y	Z
I	1.638876	2.217202	-0.876994
O	3.203167	1.345169	-1.008169
O	1.645011	2.991477	0.731909
O	2.207906	3.789233	-1.861349
H	2.927213	4.227571	-1.392465

I	0.047108	-0.140936	1.660468
O	-1.424765	0.926820	1.618775
O	0.843791	0.258916	0.072686
O	1.095476	1.117886	2.666750
H	1.312649	1.900316	2.115168
I	-3.401952	0.620074	0.341882
O	-2.335655	0.232535	-1.137462
O	-5.131298	0.380619	-0.578905
H	-5.300014	1.133343	-1.151360
I	-1.168116	-1.759971	-1.326957
O	-1.069978	-1.635326	0.555583
O	-0.063041	-3.365138	-1.418258
H	0.866112	-3.089567	-1.318258
C	4.335450	-3.200392	0.618297
H	5.030533	-3.207465	-0.215828
H	3.842428	-4.163437	0.721809
H	4.833440	-2.924774	1.543321
S	3.077614	-2.020085	0.288754
O	2.191544	-1.993737	1.421264
O	2.487423	-2.307678	-0.990669
O	3.922077	-0.745176	0.218596
H	3.516296	0.055401	-0.273325

$(HIO_3)_3(HIO_2)_1(MSA)_1$:

Atoms	X	Y	Z
I	-3.106823	-0.370436	-0.186573
O	-2.145238	-0.846587	-1.639348
O	-2.367302	1.168568	0.358986
O	-4.533365	0.501505	-1.186345
H	-4.209031	1.297354	-1.621863
I	0.061077	-2.029060	0.951439
O	-1.738609	-1.620778	1.064687
O	0.112706	-3.645227	1.641637
O	-0.024593	-2.465220	-0.911670
H	-0.820554	-2.007643	-1.267731
I	0.035066	2.050355	1.086344
O	1.860668	2.529156	1.051454
O	0.028319	0.731457	2.264618
O	-0.336960	3.459422	2.364098
H	0.015508	3.230682	3.232029
I	1.107430	0.609985	-2.134574
O	0.571602	0.435722	-0.333269
O	-0.645515	1.197801	-2.746282

H	-1.277691	0.480487	-2.534567
C	5.189397	-1.069024	-0.041490
H	5.790078	-0.188883	-0.251452
H	5.293215	-1.811758	-0.827119
H	5.449669	-1.494011	0.924183
S	3.499037	-0.583334	0.037939
O	2.724920	-1.783507	0.274350
O	3.229755	0.011272	-1.299116
O	3.397067	0.414591	1.089765
H	2.442469	1.711174	1.058207

Supplementary Reference

Almeida, J., Schobesberger, S., Kürten, A., Ortega, I. K., Kupiainen-Määttä, O., Praplan, A. P., Adamov, A., Amorim, A., Bianchi, F., Breitenlechner, M., David, A., Dommen, J., Donahue, N. M., Downard, A., Dunne, E., Duplissy, J., Ehrhart, S., Flagan, R. C., Franchin, A., Guida, R., Hakala, J., Hansel, A., Heinritzi, M., Henschel, H., Jokinen, T., Junninen, H., Kajos, M., Kangasluoma, J., Keskinen, H., Kupc, A., Kurten, T., Kvashin, A. N., Laaksonen, A., Lehtipalo, K., Leiminger, M., Leppä, J., Loukonen, V., Makhmutov, V., Mathot, S., McGrath, M. J., Nieminen, T., Olenius, T., Onnela, A., Petäjä, T., Riccobono, F., Riipinen, I., Rissanen, M., Rondo, L., Ruuskanen, T., Santos, F. D., Sarnela, N., Schallhart, S., Schnitzhofer, R., Seinfeld, J. H., Simon, M., Sipilä, M., Stozhkov, Y., Stratmann, F., Tomé, A., Tröstl, J., Tsagkogeorgas, G., Vaattovaara, P., Viisanen, Y., Virtanen, A., Vrtala, A., Wagner, P. E., Weingartner, E., Wex, H., Williamson, C., Wimmer, D., Ye, P., Yli-Juuti, T., Carslaw, K. S., Kulmala, M., Curtius, J., Baltensperger, U., Worsnop, D. R., Vehkamäki, H. and Kirkby, J.: Molecular understanding of sulphuric acid-amine particle nucleation in the atmosphere, Nature, 502, 359–363, http://doi.org/10.1038/nature12663, 2013.

Elm, J. and Kristensen, K.: Basis set convergence of the binding energies of strongly hydrogen-bonded atmospheric clusters, Phys. Chem. Chem. Phys., 19, 1122–1133, http://doi.org/10.1039/c6cp06851k, 2017.

Francl, M. M., Pietro, W. J., Hehre, W. J., Binkley, J. S., Gordon, M. S., DeFrees, D. J. and Pople, J. A.: Self-consistent molecular orbital methods. XXIII. A polarization-type basis set for second-row elements, J. Chem. Phys. , 77, 3654–3665, http://doi.org/10.1063/1.444267, 1982.

Frisch, M. J., Trucks, G. W., Schlegel, H. B., Scuseria, G. E., Robb, M. A., Cheeseman, J. R., Scalmani, G., Barone, V., Mennucci, B., Petersson, G. A., Nakatsuji, H., Caricato, M., Li, X., Hratchian, H. P., Izmaylov, A. F., Bloino, J., Zheng, G., Sonnenberg, J. L., Hada, M., Ehara, M., Toyota, K., Fukuda, R., Hasegawa, J., Ishida, M., Nakajima, T., Honda, Y., Kitao, O., Nakai, H., Vreven, T., Montgomery, J. A., Peralta, J. E., Ogliaro, F., Bearpark, M., Heyd, J. J., Brothers, E., Kudin, K. N., Staroverov, V. N., Kobayashi, R., Normand, J., Raghavachari, K., Rendell, A., Burant, J. C., Iyengar, S. S., Tomasi, J., Cossi, M., Rega, N., Millam, J. M., Klene, M., Knox, J. E., Cross, J. B., Bakken, V., Adamo, C., Jaramillo, J., Gomperts, R., Stratmann, R. E., Yazyev, O., Austin, A. J., Cammi, R., Pomelli, C., Ochterski, J. W., Martin, R. L., Morokuma, K., Zakrzewski, V. G., Voth, G. A., Salvador, P., Dannenberg, J. J., Dapprich, S., Daniels, A. D., Farkas, O., Foresman, J. B., Ortiz, J. V., Cioslowski, J. and Fox, D. J.: Gaussian 09, Revision A.02, Gaussian Inc, Wallingford CT, https://gaussian.com/g09citation/ (last access: 07 May 2022), 2009.

Froyd, K. D. and Lovejoy, E. R.: Bond energies and structures of ammonia-sulfuric acid positive cluster ions, J. Phys. Chem. A, 116, 5886-5899, http://doi.org/10.1021/jp209908f, 2012.

He, X.-C., Tham, Y. J., Dada, L., Wang, M., Finkenzeller, H., Stolzenburg, D., Iyer, S., Simon, M., ¨rten, A. K., Shen, J., Roerup, B., Rissanen, M., Schobesberger, S., Baalbaki, R., Wang, D. S., Koenig, T. K., Jokinen, T., Sarnela, N., Beck, L. J., Almeida, J., Amanatidis, S., Amorim, A., Ataei, F., Baccarini, A., Bertozzi, B., Bianchi, F., Brilke, S., Caudillo, L., Chen, D., Chiu, R., Chu, B., Dias, A., Ding, A., Dommen, J., Duplissy, J., Haddad, I. E., Carracedo, L. G., Granzin, M., Hansel, A., Heinritzi, M., Hofbauer, V., Junninen, H., Kangasluoma, J., Kemppainen, D., Kim, C., Kong, W., Krechmer, J. E., Kvashin, A., Laitinen, T., Lamkaddam, H., Lee, C. P., Lehtipalo, K., Leiminger, M., Li, Z., Makhmutov, V., Manninen, H. E., Marie, G., Marten, R., Mathot, S.,

Mauldin, R. L., Mentler, B., Moehler, O., Mueller, T., Nie, W., Onnela, A., Petaja, T., Pfeifer, J., Philippov, M., Ranjithkumar, A., Saiz-Lopez, A., Salma, I., Scholz, W., Schuchmann, S., Schulze, B., Steiner, G., Stozhkov, Y., Tauber, C., Tome, A., Thakur, R. C., Vaisanen, O., Vazquez-Pufleau, M., Wagner, A. C., Wang, Y., Weber, S. K., Winkler, P. M., Wu, Y., Xiao, M., Yan, C., Ye, Q., Ylisirnio, A., Zauner-Wieczorek, M., Zha, Q., Zhou, P., Flagan, R. C., Curtius, J., Baltensperger, U., Kulmala, M., Kerminen, V.-M., Kurten, T., Donahue, N. M., Volkamer, R., Kirkby, J., Worsnop, D. R. and Sipila, M.: Role of iodine oxoacids in atmospheric aerosol nucleation, Science, 371, 589–595, http://doi.org/10.1126/science.abe0298, 2021.

Kerminen, V.-M. and Kulmala, M.: Analytical formulae connecting the "real" and the "apparent" nucleation rate and the nuclei number concentration for atmospheric nucleation events, Journal of Aerosol Science, 33, 609-622, 2002.

Kulmala, M., Petäjä, T., Nieminen, T., Sipilä, M., Manninen, H. E., Lehtipalo, K., Dal Maso, M., Aalto, P. P., Junninen, H., Paasonen, P., Riipinen, I., Lehtinen, K. E. J., Laaksonen, A. and Kerminen, V.-M.: Measurement of the nucleation of atmospheric aerosol particles, Nature Protocols, 7, 1651-1667, http://doi.org/10.1038/nprot.2012.091, 2012.

Kupiainen, O., Ortega, I. K., Kurtén, T. and Vehkamäki, H.: Amine substitution into sulfuric acid – ammonia clusters, Atmos. Chem. Phys., 12, 3591-3599, http://doi.org/10.5194/acp-12-3591-2012, 2012.

O'Dowd, C. D., Hämeri, K., Mäkelä, J., Väkeva, M., Aalto, P., de Leeuw, G., Kunz, G. J., Becker, E., Hansson, H. C., Allen, A. G., Harrison, R. M., Berresheim, H., Kleefeld, C., Geever, M., Jennings, S. G. and Kulmala, M.: Coastal new particle formation: Environmental conditions and aerosol physicochemical characteristics during nucleation bursts, J. Geophys. Res.-Atmos., 107, http://doi.org/10.1029/2000jd000206, 2002.

Oona, K.-M. and Tinja, O.: Atmospheric Cluster Dynamics Code Technical manual, https://github.com/tolenius/ACDC/blob/main/ACDC_Manual_2020_11_25.pdf, 2020.

Peterson, K. A., Figgen, D., Goll, E., Stoll, H. and Dolg, M.: Systematically convergent basis sets with relativistic pseudopotentials. II. Small-core pseudopotentials and correlation consistent basis sets for the post-d group 16–18 elements, J. Chem. Phys. , 119, 11113–11123, http://doi.org/10.1063/1.1622924, 2003.

Rappé, A. K., Casewit, C. J., Colwell, K. S., Goddard, W. A. and Skif, W. M.: UFF, a Full Periodic Table Force Field for Molecular Mechanics and Molecular Dynamics Simulations, J. Am. Chem. Soc., 114, 10024–10035, http://doi.org/10.1021/ja00051a040, 1992.

Sipilä, M., Sarnela, N., Jokinen, T., Henschel, H., Junninen, H., Kontkanen, J., Richters, S., Kangasluoma, J., Franchin, A., peräkylä, O., Rissanen, M. P., Ehn, M., Vehkamäki, H., Kurten, T., Berndt, T., Petäjä, T., Worsnop, D., Ceburnis, D., Kerminen, V. M., Kulmala, M. and O'Dowd, C.: Molecular-scale evidence of aerosol particle formation via sequential addition of HIO_3, Nature, 537, 532–534, http://doi.org/10.1038/nature19314, 2016.

Stewart, J. J.: Optimization of parameters for semiempirical methods VI: more modifications to the NDDO approximations and re-optimization of parameters, J. Mol. Model., 19, 1–32, http://doi.org/10.1007/s00894-012-1667-x, 2013.

Stewart, J. J. P.: MOPAC 2016, Colorado Springs, CO (USA), http://openmopac.net/MOPAC2016.html, 2016.

Xia, D., Chen, J., Yu, H., Xie, H. B., Wang, Y., Wang, Z., Xu, T. and Allen, D. T.: Formation Mechanisms of Iodine-Ammonia Clusters in Polluted Coastal Areas Unveiled by Thermodynamics and

Kinetic Simulations, Environ. Sci. Technol., 54, 9235-9242, http://doi.org/10.1021/acs.est.9b07476, 2020.

Yu, H., Ren, L., Huang, X., Xie, M., He, J. and Xiao, H.: Iodine speciation and size distribution in ambient aerosols at a coastal new particle formation hotspot in China, Atmos. Chem. Phys., 19, 4025–4039, http://doi.org/10.5194/acp-19-4025-2019, 2019.

Zhang, J. and Dolg, M.: ABCluster: the artificial bee colony algorithm for cluster global optimization, Phys. Chem. Chem. Phys., 17, 24173–24181, http://doi.org/10.1039/c5cp04060d, 2015.